

Impacts of Game-Theoretic Activation on Epidemic Spread over Dynamical Networks

Ashish R. Hota, Tanya Sneh, and Kavish Gupta*

Abstract

We investigate the evolution of epidemics over dynamical networks when nodes choose to interact with others in a selfish and decentralized manner. Specifically, we analyze the susceptible-asymptomatic-infected-recovered (SAIR) epidemic in the framework of activity-driven networks with heterogeneous node degrees and time-varying activation rates, and derive both individual and degree-based mean-field approximations of the exact state evolution. We then present a game-theoretic model where nodes choose their activation probabilities in a strategic manner using current state information as feedback, and characterize the *quantal response equilibrium* (QRE) of the proposed setting. We then consider the activity-driven susceptible-infected-susceptible (SIS) epidemic model, characterize equilibrium activation probabilities and analyze epidemic evolution in closed-loop. Our numerical results provide compelling insights into epidemic evolution under game-theoretic activation. Specifically, for the SAIR epidemic, we show that under suitable conditions, the epidemic can persist, as any decrease in infected proportion is counteracted by an increase in activity rates by the nodes. For the SIS epidemic, we show that in regimes where there is an endemic state, the infected proportion could be significantly smaller under game-theoretic activation if the loss upon infection is sufficiently high.

1 Introduction

Infectious diseases exploit the interaction among human beings and spread through society, sometimes infecting millions of people across the globe within a few months. In the absence of effective medicines and vaccines, reducing the social interaction between individuals is critical to contain the spread of highly infectious diseases. As observed in the context of COVID-19, Governments across the world have imposed various restrictions on human interaction and travel in the hopes of containing the spread of the epidemic and to save lives, often incurring significant economic distress [Coibion et al., 2020]. However, the success of these measures depends critically on whether individuals or groups comply with them. It is often infeasible for Governments to perfectly enforce these restrictions, and as observed in case of COVID-19, there have been instances where the infections have grown during periods of lockdown while in different regions of the world, infections have been contained in the absence of any significant restrictions on human mobility [Dahlberg et al., 2020, Pachetti et al., 2020].

Therefore, it is critical to understand how humans make decisions regarding their level of interaction during the spread of an epidemic and the impacts of such decisions on the evolution of the epidemic. In this work, we rigorously investigate this problem by modeling (i) the evolution of the epidemic in the framework of activity-driven networks and (ii) the human decision-making process in a game-theoretic framework that allows the decision-makers to have bounded rationality.

*The authors are with the Department of Electrical Engineering, IIT Kharagpur. Email: ahota@ee.iitkgp.ac.in, tanyasneh@gmail.com, kavishgupta1999@gmail.com.

1.1 Related work

The susceptible-infected-recovered (SIR) and susceptible-infected-susceptible (SIS) epidemic models remain as two fundamental mathematical models of epidemic dynamics [Hethcote, 2000, Nowzari et al., 2016, Pastor-Satorras et al., 2015]. In both epidemic models, susceptible nodes become infected in a probabilistic manner if they come in contact with infected nodes. While in the SIR epidemic, an infected node develops immunity from the disease, in the SIS epidemic, there is a possibility of re-infection. Much of the prior work has investigated the above two epidemic dynamics (including developing mean-field approximations, analyzing equilibrium behavior, centralized resource allocation for containing epidemics, among others) on well-mixed populations and on static networks [Pastor-Satorras et al., 2015]. However, the contact pattern in human society is dynamic and time-varying. Furthermore, during the prevalence of an epidemic, people modify their interaction patterns in order to protect themselves from becoming infected. In other words, the network evolves in a time-scale that is comparable to the evolution of the epidemic and in an adaptive manner (i.e., the changes occur in response to the epidemic states). Accordingly, several recent works have focused on understanding epidemic dynamics on temporal or dynamical networks [Enright and Kao, 2018, Masuda and Holme, 2017, Paré et al., 2017].

In this work, we consider the framework of activity-driven networks (ADNs) where the epidemic states and network topology evolves in a comparable time-scale [Masuda and Holme, 2017, Perra et al., 2012, Zino et al., 2017]. In the framework of ADNs, nodes activate with a certain probability (possibly depending on their epidemic state) and form connections with other nodes at random. Once the connections are formed, the epidemic states of the nodes changes according to the SIR or SIS model. Eventually, the connections are discarded. Several recent papers have investigated SIR and SIS epidemics on ADNs. Specifically, [Nadini et al., 2020, Zino et al., 2020a,b] consider continuous-time evolution of epidemic states and network topology, investigate the impact of self-activation rates where infected nodes reduce their activity (potentially due to sickness) and derive conditions under which the epidemic is eradicated. In contrast, [Ogura et al., 2019] considers discrete-time and adaptive evolution of the SIS epidemic on ADNs, derives mean-field approximations and computes optimal interventions under which the epidemic is eradicated. The above settings assume that (i) all nodes are (degree) homogeneous (i.e., they choose the same number of nodes to connect to upon activation), (ii) nodes activate at a reduced rate without any strategic (game-theoretic) decision-making, (iii) optimal activity rates are computed via centralized optimization, and (iv) the impacts of asymptomatic carriers (as is the case with COVID-19) are not considered. In our prior work [Hota and Gupta, 2020], we generalized the setting in [Ogura et al., 2019] to include asymptomatic carriers and degree heterogeneity in the SIS epidemic model and derived an accurate bound on the decay ratio.

In contrast with the above works where the activity rates are specified in an exogenous manner or optimized by a central authority, humans take these decisions in a selfish and decentralized manner by evaluating the (social and economic) benefits of such interactions with the possible risk of becoming infected. Therefore, in this paper, we propose a game-theoretic framework where nodes choose their activation probabilities in order to maximize a suitably defined state-dependent utility function. Earlier work on game-theoretic reduction in contact rates has primarily focused on the setting with a well-mixed population [Bauch and Earn, 2004, Chang et al., 2020, Choi and Shim, 2020, Fenichel et al., 2011, Reluga, 2010, Theodorakopoulos et al., 2013]. Recent papers have analyzed the impacts of game-theoretic protection against networked epidemic models [Hota and Sundaram, 2019a,b, Omic et al., 2009, Trajanovski et al., 2018]. Most of the above works focus on the classical SIS epidemic model (on static networks) and define the cost in terms of the infection probability at the endemic state of the SIS epidemic under a mean-field approximation.

In other words, decisions are made over a longer time-scale compared to the epidemic evolution. In a related work [Huang and Zhu, 2020], the authors consider a differential game framework for the SIS epidemic. A few recent works consider game-theoretic models of social distancing in a comparable time-scale as epidemic evolution; specifically [Cho, 2020, Dasaratha, 2020] consider adaptive activation rates in well-mixed populations while [Lagos et al., 2020] studies the impacts of local and aggregate information on the equilibrium strategies in a networked SIR epidemic model.

To the best of our knowledge, ours is one of the first papers to rigorously analyze game-theoretic or strategic choice of activation rates in temporal networks, particularly in the ADN framework that (i) incorporates bounded rationality in decision-making, (ii) heterogeneous node degrees, and (iii) asymptomatic carriers. We now summarize the contributions of this work.

1.2 Summary of contributions

We first define an activity-driven and adaptive analogue of the susceptible-asymptomatic-infected-recovered (SAIR) epidemic model [Ansumalia et al., 2020, Robinson and Stilianakis, 2013, Stella et al., 2020] (Section 2). In the SAIR epidemic, nodes in the asymptomatic state can cause new infections and can potentially recover without ever exhibiting symptoms. Consequently, this is an appropriate framework to model diseases such as COVID-19 (compared to the classical SIR epidemic model) [Ansumalia et al., 2020]. Furthermore, both SIR and SEIR (with state E pertaining to the exposed state) models are special cases of the SAIR epidemic model as we show later. We consider a discrete-time model of epidemic and network evolution analogous to the setting in [Ogura et al., 2019], and refer our model as the A-SAIR epidemic. We relax the homogeneity assumption prevalent in prior works and assume that all nodes, upon activation, choose potentially different number of nodes to connect to. We then derive individual-based and degree-based mean-field approximations of the exact Markovian evolution of the epidemic under arbitrary state and time-dependent activation rates.

In Section 3, we formally introduce the *activation game* where each node decides whether to activate or not at each time. Nodes who activate receive a benefit, while susceptible nodes experience a risk of becoming infected due to their interactions. We assume that nodes in the asymptomatic state are not aware of being infected and continue to behave as susceptible nodes. Symptomatic nodes no longer face the risk of becoming infected, but incur a higher cost if they activate. We assume that nodes choose their actions according to the logit choice model which captures bounded rationality prevalent in human decision-making [Greene, 2009, Luce, 1958], and consider the notion of quantal response equilibrium (QRE) [McKelvey and Palfrey, 1995] as the solution concept. The QRE is a generalization of the Nash equilibrium which allows for stochastic uncertainty in the utility functions of the nodes, has strong behavioral foundations and has been shown to explain/predict observed human behavior in many applications [Goeree et al., 2002, 2020, Haile et al., 2008, McKelvey and Palfrey, 1995].

We define the infection risk of the nodes via (degree-based) mean-field approximations and characterize the activation probabilities of the nodes at the QRE in the A-SAIR epidemic model. Specifically, we show that, under suitable assumptions, the equilibrium activation probability for susceptible and asymptomatic nodes is a function of the proportion of asymptomatic and symptomatic nodes in the network, i.e., nodes use information regarding the current epidemic prevalence as feedback to determine their activity rates.

In Section 4, we consider the activity-driven SIS epidemic model, derive the individual and degree-based mean-field approximations of the exact epidemic dynamic and characterize the activation probabilities of the nodes at the QRE; the latter being a nonlinear function of the current epidemic prevalence. We then analyze the nonlinear closed-loop dynamics under game-theoretic

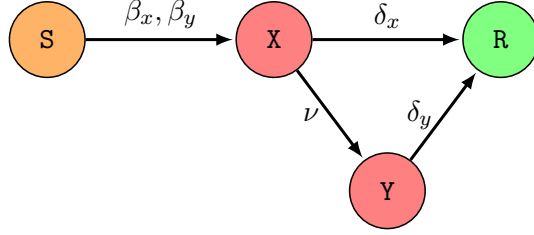


Figure 1: Probabilistic evolution of states in the A-SAIR epidemic model. Self-loops are omitted for better clarity. See Definition 1 for the formal definition. Red indicates that both X and Y are infected (as well as infectious) states.

activation probabilities in several special cases of interest.

Finally, in Section 5, we report extensive simulations of the evolution of the epidemic states under game-theoretic activation decisions. Our results highlight the accuracy of the mean-field approximations and the impacts of asymptomatic carriers and heterogeneity in degree distributions on the evolution of the A-SAIR epidemic. Specifically, we show that under certain conditions, selfish and decentralized activation decisions can lead to long-term persistence of the disease in the population because any decline in the infected population is counteracted by an increase in activation probabilities, and vice versa. In addition, networks with a power-law degree distribution may see a higher peak in the infected population as nodes with a smaller degree experience a smaller infection risk and consequently, may not decrease their activity rates. For the A-SIS epidemic, we show that if the loss due to infection is sufficiently high, the proportion of infected nodes at the endemic state can be made arbitrarily small under game-theoretic activation. We conclude with a discussion on directions for future research.

2 Activity-Driven Adaptive SAIR Epidemic Model

In this section, we formally define the activity-driven adaptive SAIR (A-SAIR) epidemic model and approximate the probabilistic evolution of the epidemic states via individual-based and degree-based mean-field (DBMF) approximations. Let $\mathcal{V} = \{v_1, v_2, \dots, v_n\}$ denote the set of n nodes. Each node remains in one of the four possible states: susceptible (S), asymptomatic (X), infected with symptoms or symptomatic (Y) and recovered (R). We assume that the recovered state includes the nodes that are deceased. Both asymptomatic and symptomatic individuals are infectious, which captures the characteristics of epidemics such as COVID-19. The states evolve in discrete-time. If at time $k \in \{0, 1, \dots\}$, node v_i is susceptible (respectively, asymptomatic, symptomatic and recovered), we denote this by $v_i(k) \in \mathbf{S}$ (respectively, $v_i(k) \in \mathbf{X}$, $v_i(k) \in \mathbf{Y}$ and $v_i(k) \in \mathbf{R}$). Given a network or contact pattern, the probabilistic state evolution is defined below.

Definition 1. Let $\beta_x, \beta_y, \delta_x, \delta_y, \nu \in [0, 1]$ be constants pertaining to infection, recovery and transition rates. The state of each node v_i evolves as follows.

1. If $v_i(k) \in \mathbf{S}$, then $v_i(k+1) \in \mathbf{X}$ with probability β_x for each asymptomatic neighbor and with probability β_y for each symptomatic neighbor independently of other neighbors.
2. If $v_i(k) \in \mathbf{X}$, then $v_i(k+1) \in \mathbf{R}$ with probability δ_x and $v_i(k+1) \in \mathbf{Y}$ with probability $\nu(1 - \delta_x)$.
3. If $v_i(k) \in \mathbf{Y}$, then $v_i(k+1) \in \mathbf{R}$ with probability δ_y .

The state remains unchanged otherwise. □

The possible transitions of the states are illustrated in Figure 1. Thus, in our model, both asymptomatic and symptomatic nodes can potentially infect a susceptible node, albeit with possibly different probabilities (β_x and β_y , respectively). Upon being infected, a susceptible node becomes asymptomatic. From there on, it can either get cured and become recovered with probability δ_x , and if not, it transitions to the symptomatic state with probability ν . Thus ν^{-1} captures the delay in onset of symptoms. The recovery/curing rate for symptomatic nodes is δ_y . Thus, in our model, a node can get infected and cured without ever exhibiting symptoms. Nodes in state **X** act as asymptomatic carriers of the disease.

We denote the degree of node v_i as $d_i \in \mathcal{D}$ where $\mathcal{D} \subset \{1, 2, \dots, d_{\max}\}$ denotes the set of all degrees of the nodes. The maximum degree d_{\max} is assumed to be finite. The proportion of nodes with degree $d \in \mathcal{D}$ is denoted by m_d with $\sum_{d \in \mathcal{D}} m_d = 1$. We denote the average or mean degree by $d_{\text{avg}} := \sum_{d \in \mathcal{D}} dm_d$. We now formally define the state-dependent evolution of the network or contact pattern for our setting.

Definition 2. For each node $v_i \in \mathcal{V}$, let $\pi_{\mathbf{Z},i}(k) \in [0, 1]$ denote the activation probability of node v_i at time k in state $\mathbf{Z} \in \{\mathbf{S}, \mathbf{X}, \mathbf{Y}, \mathbf{R}\}$. Let $\beta_x, \beta_y, \delta_x, \delta_y, \nu \in [0, 1]$ be constants pertaining to infection, recovery and transition rates. The A-SAIR model is defined by the following procedures:

1. At the initial time $k = 0$, each node is in one of the four possible states.
2. At each time $k = 1, 2, \dots$, each node v_i activates with probability $\pi_{\mathbf{Z},i}(k)$ where \mathbf{Z} is the state of v_i at k independently of other nodes .
3. Node v_i , upon activation, chooses d_i other nodes randomly and uniformly among all nodes and forms edges with them. If v_j is chosen by v_i , an (undirected) edge (v_i, v_j) is created with probability 1.
4. Once the edges are formed, the states of the nodes get updated following Definition 1.
5. These edges are discarded at time $k + 1$. Steps 2-4 are repeated for each time $k \geq 1$. □

Note that the activation probabilities are potentially time-varying, state-dependent and heterogeneous across nodes. The following remark highlights the generality of the proposed model.

Remark 1. The above model captures several epidemic models as special cases.

1. When $\beta_x = \delta_x = 0$, then nodes in asymptomatic state **X** necessarily become symptomatic before recovering. Furthermore, nodes in **X** do not cause any new infections. Thus, we recover the activity-driven analogue of the classical SEIR epidemic model with nodes in **X** being analogous to the “exposed” state in the SEIR model.
2. When $\nu = 0$ and none of the nodes are in state **Y** at time $k = 0$, we recover the activity-driven analogue of the classical SIR epidemic with **X** being the state of infected nodes. □

We now analyze the state evolution and derive mean-field approximations of the above general model which will enable us to obtain valuable insights on epidemic evolution in large-scale networks. Subsequently, we consider a setting where nodes choose these activation probabilities in a selfish and decentralized manner to maximize their individual utility functions at each time step.

2.1 State Evolution and Mean-Field Approximations

In order to analyze the evolution of the states in the A-SAIR epidemic model, we define (indicator) random variables $S_i(k), X_i(k), Y_i(k)$ and $R_i(k)$ associated with node v_i that take values in the set $\{0, 1\}$. Specifically, we define $S_i(k) = 1$ if $v_i(k) \in \mathbf{S}$, $X_i(k) = 1$ if $v_i(k) \in \mathbf{X}$, $Y_i(k) = 1$ if $v_i(k) \in \mathbf{Y}$ and $R_i(k) = 1$ if $v_i(k) \in \mathbf{R}$. Since a node can only be in one of the four possible states, we have $S_i(k) + X_i(k) + Y_i(k) + R_i(k) = 1$. Similarly, we define a $\{0, 1\}$ -valued random variable $A_{ij}(k)$ which takes value 1 if the edge (v_i, v_j) exists at time k . We also denote by N_x a Bernoulli random variable that takes value 1 with probability $x \in [0, 1]$. The exact state evolution of a node v_i under the A-SAIR epidemic model can now be formally stated as:

$$S_i(k+1) = S_i(k) \prod_{j \neq i} [1 - A_{ij}(k)(X_j(k)N_{\beta_x} + Y_j(k)N_{\beta_y})], \quad (1a)$$

$$\begin{aligned} X_i(k+1) &= (1 - N_{\delta_x})(1 - N_{\nu})X_i(k) \\ &\quad + S_i(k) \left[1 - \prod_{j \neq i} [1 - A_{ij}(k)(X_j(k)N_{\beta_x} + Y_j(k)N_{\beta_y})] \right], \end{aligned} \quad (1b)$$

$$Y_i(k+1) = (1 - N_{\delta_x})N_{\nu}X_i(k) + (1 - N_{\delta_y})Y_i(k), \quad (1c)$$

$$R_i(k+1) = R_i(k) + N_{\delta_x}X_i(k) + N_{\delta_y}Y_i(k). \quad (1d)$$

It is easy to see that $S_i(k+1) + X_i(k+1) + Y_i(k+1) + R_i(k+1) = S_i(k) + X_i(k) + Y_i(k) + R_i(k) = 1$. We denote the probability of node v_i being susceptible at time k by $s_i(k)$, i.e., $s_i(k) := \mathbb{P}(v_i(k) \in \mathbf{S}) = \mathbb{P}(S_i(k) = 1) = \mathbb{E}[S_i(k)]$. Similarly, we define $x_i(k) := \mathbb{P}(X_i(k) = 1) = \mathbb{E}[X_i(k)]$, $y_i(k) := \mathbb{P}(Y_i(k) = 1) = \mathbb{E}[Y_i(k)]$ and $r_i(k) := \mathbb{P}(R_i(k) = 1) = \mathbb{E}[R_i(k)]$.

Note that the infection states follow a Markov process with a $4^n \times 4^n$ transition probability matrix. While analyzing the exact state evolution of this model is computationally intractable, we first present a mean-field approximation of the evolution of the epidemic states for each individual node.

Theorem 1 (Individual-based mean-field approximation of the A-SAIR epidemic). *Consider the A-SAIR epidemic model defined in Definition 2. Let $\bar{d}_i = d_i/(n-1)$, and for all i, j , define the constants*

$$\beta_x^{ij}(k) := \beta_x [1 - (1 - \pi_{\mathbf{S},i}(k)\bar{d}_i)(1 - \pi_{\mathbf{X},j}(k)\bar{d}_j)], \quad (2)$$

$$\beta_y^{ij}(k) := \beta_y [1 - (1 - \pi_{\mathbf{S},i}(k)\bar{d}_i)(1 - \pi_{\mathbf{Y},j}(k)\bar{d}_j)]. \quad (3)$$

Then,

$$s_i(k+1) \simeq s_i(k) \left(1 - \sum_{j \neq i} [\beta_x^{ij}(k)x_j(k) + \beta_y^{ij}(k)y_j(k)] \right), \quad (4a)$$

$$x_i(k+1) \simeq \delta_x^c(1 - \nu)x_i(k) + s_i(k) \sum_{j \neq i} [\beta_x^{ij}(k)x_j(k) + \beta_y^{ij}(k)y_j(k)], \quad (4b)$$

$$y_i(k+1) = \delta_x^c \nu x_i(k) + (1 - \delta_y)y_i(k), \quad (4c)$$

$$r_i(k+1) = r_i(k) + \delta_x x_i(k) + \delta_y y_i(k), \quad (4d)$$

for all nodes v_i and $k \geq 0$ with $\delta_x^c = 1 - \delta_x$. □

Proof. We compute expectation on both sides of (1b) and (1c) and obtain

$$x_i(k+1) = \delta_x^c(1 - \nu)x_i(k)$$

$$+ \mathbb{E} \left[S_i(k) \left[1 - \prod_{j \neq i} \left[1 - A_{ij}(k) (X_j(k) N_{\beta_x} + Y_j(k) N_{\beta_y}) \right] \right] \right], \quad (5a)$$

$$y_i(k+1) = \delta_x^c \nu x_i(k) + (1 - \delta_y) y_i(k), \quad (5b)$$

For the product term in the R.H.S. of (5a), the Weierstrass product inequality yields

$$1 - \prod_{j \neq i} \left[1 - A_{ij}(k) (X_j(k) N_{\beta_x} + Y_j(k) N_{\beta_y}) \right] \leq \sum_{j \neq i} A_{ij}(k) (X_j(k) N_{\beta_x} + Y_j(k) N_{\beta_y}).$$

Consequently, we have

$$\begin{aligned} & \mathbb{E} \left[S_i(k) \left[1 - \prod_{j \neq i} \left[1 - A_{ij}(k) (X_j(k) N_{\beta_x} + Y_j(k) N_{\beta_y}) \right] \right] \right] \\ & \leq \sum_{j \neq i} \beta_x \mathbb{E} [A_{ij}(k) S_i(k) X_j(k)] + \beta_y \mathbb{E} [A_{ij}(k) S_i(k) Y_j(k)]. \end{aligned} \quad (6)$$

We now focus on evaluating the expectation terms in the above equation. Recall that $A_{ij}(k)$ is a random variable that indicates the presence of the edge (v_i, v_j) at time k and is governed by the states and activation probabilities of nodes v_i and v_j according to Definition 2. In order to compute the expectation terms, we introduce the following notation for events of interest:

$$\mathbf{SX}_{ij}^k = "v_i(k) \in \mathbf{S} \text{ and } v_j(k) \in \mathbf{X}," \quad (7)$$

$$\mathbf{SY}_{ij}^k = "v_i(k) \in \mathbf{S} \text{ and } v_j(k) \in \mathbf{Y}," \quad (8)$$

$$\Gamma_{i \rightarrow j}^k = "v_i \text{ is activated, and chooses } v_j \text{ as neighbor at time } k." \quad (9)$$

With the above notation in place, we have

$$\begin{aligned} \mathbb{E} [A_{ij}(k) S_i(k) X_j(k)] &= \mathbb{P}(A_{ij}(k) = 1, S_i(k) = 1, X_j(k) = 1) \\ &= \mathbb{P}(A_{ij}(k) = 1 | \mathbf{SX}_{ij}^k) \mathbb{P}(\mathbf{SX}_{ij}^k), \end{aligned} \quad (10a)$$

$$\mathbb{E} [A_{ij}(k) S_i(k) Y_j(k)] = \mathbb{P}(A_{ij}(k) = 1 | \mathbf{SY}_{ij}^k) \mathbb{P}(\mathbf{SY}_{ij}^k). \quad (10b)$$

We now focus on the first equation above and note that

$$\begin{aligned} \mathbb{P}(A_{ij}(k) = 1 | \mathbf{SX}_{ij}^k) &= \mathbb{P}(\Gamma_{i \rightarrow j}^k \cup \Gamma_{j \rightarrow i}^k | \mathbf{SX}_{ij}^k) \\ &= \mathbb{P}(\Gamma_{i \rightarrow j}^k | \mathbf{SX}_{ij}^k) + \mathbb{P}(\Gamma_{j \rightarrow i}^k | \mathbf{SX}_{ij}^k) - \mathbb{P}(\Gamma_{i \rightarrow j}^k | \mathbf{SX}_{ij}^k) \mathbb{P}(\Gamma_{j \rightarrow i}^k | \mathbf{SX}_{ij}^k) \\ &= 1 - [1 - \mathbb{P}(\Gamma_{i \rightarrow j}^k | \mathbf{SX}_{ij}^k)] [1 - \mathbb{P}(\Gamma_{j \rightarrow i}^k | \mathbf{SX}_{ij}^k)] \\ &= 1 - [1 - \pi_{\mathbf{S},i}(k) \bar{d}_i] [1 - \pi_{\mathbf{X},j}(k) \bar{d}_j] \end{aligned}$$

following Definition 2. Note that the probability of an activated node v_i choosing a specific node v_j is $\bar{d}_i = \frac{d_i}{n-1}$. Similarly for events conditioned on \mathbf{SY}_{ij}^k , we have

$$\begin{aligned} \mathbb{P}(A_{ij}(k) = 1 | \mathbf{SY}_{ij}^k) &= 1 - [1 - \mathbb{P}(\Gamma_{i \rightarrow j}^k | \mathbf{SY}_{ij}^k)] [1 - \mathbb{P}(\Gamma_{j \rightarrow i}^k | \mathbf{SY}_{ij}^k)] \\ &= 1 - [1 - \pi_{\mathbf{S},i}(k) \bar{d}_i] [1 - \pi_{\mathbf{Y},j}(k) \bar{d}_j]. \end{aligned}$$

Finally, we approximate $\mathbb{P}(\mathbf{SX}_{ij}^k)$ and $\mathbb{P}(\mathbf{SY}_{ij}^k)$ by assuming that the events $v_i(k) \in \mathbf{S}$ and $v_j(k) \in \mathbf{X}$ (or $v_j(k) \in \mathbf{Y}$) are independent. Substituting the above in (10), we obtain

$$\mathbb{E} [A_{ij}(k) S_i(k) X_j(k)] = [1 - [1 - \pi_{\mathbf{S},i}(k) \bar{d}_i] [1 - \pi_{\mathbf{X},j}(k) \bar{d}_j]] \mathbb{P}(\mathbf{SX}_{ij}^k)$$

$$\begin{aligned} &\simeq [1 - [1 - \pi_{\mathbf{S},i}(k)\bar{d}_i][1 - \pi_{\mathbf{X},j}(k)\bar{d}_j]]s_i(k)x_j(k), \\ \mathbb{E}[A_{ij}(k)S_i(k)Y_j(k)] &\simeq [1 - [1 - \pi_{\mathbf{S},i}(k)\bar{d}_i][1 - \pi_{\mathbf{Y},j}(k)\bar{d}_j]]s_i(k)y_j(k). \end{aligned}$$

The result now follows upon substituting the above expressions in (6) using the definition of β_x^{ij} and β_y^{ij} , and taking expectations on both sides of (1a) and (1d). This concludes the proof. \square

The result shows that the evolution of the probability of a node being in any of the four epidemic states is approximated by the dynamics stated in (4) with state dimension $4n$ which is considerably smaller than the exact Markovian evolution with dimension 4^n .

We now leverage the above result to obtain a degree-based mean field (DBMF) approximation of the A-SAIR epidemic model when all nodes of a given degree behave in an identical manner. Specifically, we assume that all nodes with a given degree choose an identical state-dependent activation probability and are equally likely to be in any of the epidemic states. The accuracy of the DBMF approximation improves when the number of nodes increases.

Definition 3. Consider the A-SAIR epidemic model defined in Definition 2. Let all nodes with degree $d \in \mathcal{D}$ choose an identical (state-dependent) activation probability denoted by $\pi_{d,\mathbf{Z}}(k)$ with $\mathbf{Z} \in \{\mathbf{S}, \mathbf{X}, \mathbf{Y}, \mathbf{R}\}$. Let $\bar{d} = d/(n-1)$, and for all $d, t \in \mathcal{D}$, define the constants

$$\beta_x^{dt}(k) := \beta_x[1 - (1 - \pi_{d,\mathbf{S}}(k)\bar{d})(1 - \pi_{t,\mathbf{X}}(k)\bar{t})], \quad (11)$$

$$\beta_y^{dt}(k) := \beta_y[1 - (1 - \pi_{d,\mathbf{S}}(k)\bar{d})(1 - \pi_{t,\mathbf{Y}}(k)\bar{t})]. \quad (12)$$

Let $s_d(k), x_d(k), y_d(k), r_d(k)$ denote the proportion of degree d nodes that are susceptible, asymptomatic, symptomatic and recovered at time k , respectively. Then, we define the DBMF approximation of the A-SAIR epidemic as the dynamics given by

$$s_d(k+1) = s_d(k) \left(1 - \sum_{t \in \mathcal{D}} nm_t [\beta_x^{dt}(k)x_t(k) + \beta_y^{dt}(k)y_t(k)] \right), \quad (13a)$$

$$x_d(k+1) = \delta_x^c(1 - \nu)x_d(k) + s_d(k) \sum_{t \in \mathcal{D}} nm_t [\beta_x^{dt}(k)x_t(k) + \beta_y^{dt}(k)y_t(k)], \quad (13b)$$

$$y_d(k+1) = \delta_x^c \nu x_d(k) + (1 - \delta_y)y_d(k), \quad (13c)$$

$$r_d(k+1) = r_d(k) + \delta_x x_d(k) + \delta_y y_d(k), \quad (13d)$$

for all degrees d and $k \geq 0$ with $\delta_x^c = 1 - \delta_x$. \square

The above approximation is inspired by the analysis in Theorem 1. Specifically, we have assumed that all nodes with a given degree have an identical activation probability and are equally likely to be in any given state. Accordingly, for a node v_i with degree d , we have

$$\sum_{j \neq i} [\beta_x^{ij}(k)x_j(k) + \beta_y^{ij}(k)y_j(k)] \simeq \sum_{t \in \mathcal{D}} nm_t [\beta_x^{dt}(k)x_t(k) + \beta_y^{dt}(k)y_t(k)],$$

as all nodes with degree t contribute an identical quantity in the summation and the number of nodes with degree t is nm_t .

Note that when we treat all nodes with a given degree d to have an identical activation probability, we denote the activation probability as $\pi_{d,\mathbf{Z}}$ while when we consider the activation probability of a node v_i , we denote it as $\pi_{\mathbf{Z},i}$.

We will rely on the DBMF approximation in the following section when we analyze strategic activation decisions by the nodes. We illustrate the accuracy of the DBMF approximation via simulations in Section 5.

Remark 2. *The dynamics under the mean-field approximations ((4) and (13)) indicate that the probability of a node being susceptible or the proportion of susceptible nodes is monotonically decreasing and any equilibrium must be free from infected nodes. When the activation probabilities are constants, the dynamics ((4) and (13)) are analogous to the dynamics of the classical SAIR epidemic. The equilibrium behavior in this setting was recently analyzed in [Ansumalia et al., 2020, Paré et al., 2020a, Stella et al., 2020] along with a discussion on open problems. We omit further discussions on this as it is not a major contribution of our work. \square*

3 To Activate or Not: Game-Theoretic Model

In this section, we formulate and analyze a game-theoretic setting where nodes choose their activation probabilities in a selfish and decentralized manner.

We consider the A-SAIR epidemic model described above. At the beginning of time k , nodes decide whether to activate themselves or not in order to maximize their individual utilities at time k in a myopic manner. The utility of a node is a function of its epidemic state, its chosen action and the states and actions of other nodes. Since the network is randomly created anew at each time step, all nodes with a given degree and epidemic state face an identical decision problem and as a result, we assume that all nodes of a given degree and state adopt the same strategy. This enables us to characterize the equilibrium behavior and epidemic evolution in large-scale networks in a scalable manner. We refer the collection of nodes with degree $d \in \mathcal{D}$ as a subpopulation with degree d .

We now define the utility of a node in different epidemic states. We assume that if a node activates, it receives 1 unit of benefit irrespective of its epidemic state; this potentially captures benefits due to social and economic interactions the node is expected to have by activating itself. In addition, we assume that a symptomatically infected node incurs a cost $c \in \mathbb{R}_+$ if it activates itself, which captures, for instance, deterrent placed by authorities for violating quarantine rules. If the node is susceptible, there is a risk that it will get infected when it comes in contact with another infected node and incurs a loss $L \in \mathbb{R}_+$ if it becomes infected. An asymptomatic node is unaware of its infection state and as a result, behaves as a susceptible node. Nodes in symptomatic and recovered states do not incur any risk of infection.

Formally, a strategy profile for the nodes is denoted by $\pi := \{\pi_S, \pi_X, \pi_Y, \pi_R\}$ with $\pi_Z := \{\pi_{d,Z}\}_{d \in \mathcal{D}} \subseteq [0, 1]^{|\mathcal{D}|}$ where $\pi_{d,Z} \in [0, 1]$ denotes the activation probability of a node with degree d in epidemic state $Z \in \{S, X, Y, R\}$. If a node decides to activate, we denote its action as A; the decision to not activate is denoted as N. At time k , we denote the global epidemic state as $e(k) := \{s_d(k), x_d(k), y_d(k), r_d(k)\}_{d \in \mathcal{D}}$, i.e, the proportion of nodes in each epidemic state in each subpopulation. We assume that at a given time k , nodes are aware of the epidemic state either completely or at an aggregate level (to be made precise subsequently). The information available to the nodes regarding the epidemic state is denoted as $\bar{e}(k)$. The utility of a node v with degree $d \in \mathcal{D}$ in different epidemic states at time k are defined as:

$$u_{d,S}(\mathbf{A}, \pi, \bar{e}(k)) = 1 - L\mathbb{R}_d(\pi, \bar{e}(k)|v(k) \in \mathbf{SA}), \quad (14a)$$

$$u_{d,S}(\mathbf{N}, \pi, \bar{e}(k)) = -L\mathbb{R}_d(\pi, \bar{e}(k)|v(k) \in \mathbf{SN}), \quad (14b)$$

$$u_{d,X}(\mathbf{A}, \pi, \bar{e}(k)) = u_{d,S}(\mathbf{A}, \pi, \bar{e}(k)), \quad u_{d,X}(\mathbf{N}, \pi, \bar{e}(k)) = u_{d,S}(\mathbf{N}, \pi, \bar{e}(k)), \quad (14c)$$

$$u_{d,Y}(\mathbf{A}, \pi, \bar{e}(k)) = 1 - c, \quad u_{d,Y}(\mathbf{N}, \pi, \bar{e}(k)) = 0, \quad (14d)$$

$$u_{d,R}(\mathbf{A}, \pi, \bar{e}(k)) = 1, \quad u_{d,R}(\mathbf{N}, \pi, \bar{e}(k)) = 0, \quad (14e)$$

where $\mathbb{R}_d(\pi, \bar{e}(k)|v(k) \in \mathbf{SA})$ (respectively, $\mathbb{R}_d(\pi, \bar{e}(k)|v(k) \in \mathbf{SN})$) denotes the risk factor for a susceptible node of degree d under strategy profile π if it activates (respectively, does not activate)

denoted by **SA** (respectively, **SN**). We refer the above game-theoretic setting as the *activation game*. We now define the individual choice model and the notion of equilibrium in the proposed setting. Subsequently, we will make the notion of risk factor precise.

We assume that nodes choose their actions in a probabilistic manner following the logit choice model. Specifically, in epidemic state **Z**, a node with degree d chooses action **A** with probability

$$\sigma_{d,Z,A}^\lambda(\pi, \bar{e}(k)) = \frac{e^{\lambda u_{d,z}(\mathbf{A}, \pi, \bar{e}(k))}}{e^{\lambda u_{d,z}(\mathbf{A}, \pi, \bar{e}(k))} + e^{\lambda u_{d,z}(\mathbf{N}, \pi, \bar{e}(k))}}, \quad \mathbf{Z} \in \{\mathbf{S}, \mathbf{X}, \mathbf{Y}, \mathbf{R}\}, d \in \mathcal{D}, \quad (15)$$

where the parameter λ captures the error in decision-making process of the nodes. As $\lambda \rightarrow 0$, both actions are chosen with probabilities approaching 0.5 (nodes choose their actions completely randomly) while as $\lambda \rightarrow \infty$, the action with higher utility is chosen with probability approaching 1 (nodes are perfectly rational). Intermediate values of λ capture bounded rationality in the decisions made by the nodes [McKelvey and Palfrey, 1995]. We now formally define the notion of a quantal response equilibrium in this game.

Definition 4. A strategy profile $\pi_{\mathbf{NE}}^\lambda(k) = \{\pi_{\mathbf{S},\mathbf{NE}}^\lambda(k), \pi_{\mathbf{X},\mathbf{NE}}^\lambda(k), \pi_{\mathbf{Y},\mathbf{NE}}^\lambda(k), \pi_{\mathbf{R},\mathbf{NE}}^\lambda(k)\}$ is a quantal response equilibrium (QRE) with parameter λ at time k if

$$\begin{aligned} \pi_{d,Z,\mathbf{NE}}^\lambda(k) &= \sigma_{d,Z,\mathbf{A}}^\lambda(\pi_{\mathbf{NE}}^\lambda(k), \bar{e}(k)) \\ &= \frac{e^{\lambda u_{d,z}(\mathbf{A}, \pi_{\mathbf{NE}}^\lambda(k), \bar{e}(k))}}{e^{\lambda u_{d,z}(\mathbf{A}, \pi_{\mathbf{NE}}^\lambda(k), \bar{e}(k))} + e^{\lambda u_{d,z}(\mathbf{N}, \pi_{\mathbf{NE}}^\lambda(k), \bar{e}(k))}} \\ &= \frac{e^{\lambda \Delta u_{d,z}(\pi_{\mathbf{NE}}^\lambda(k), \bar{e}(k))}}{e^{\lambda \Delta u_{d,z}(\pi_{\mathbf{NE}}^\lambda(k), \bar{e}(k))} + 1}, \end{aligned}$$

where $\Delta u_{d,z}(\pi, \bar{e}(k)) := u_{d,z}(\mathbf{A}, \pi, \bar{e}(k)) - u_{d,z}(\mathbf{N}, \pi, \bar{e}(k))$ for $\mathbf{Z} \in \{\mathbf{S}, \mathbf{X}, \mathbf{Y}, \mathbf{R}\}, d \in \mathcal{D}$. \square

The above definition is essentially a consistency condition: the probability with which a node activates under the logistic quantal response model coincides with the equilibrium strategy. Since there is a finite number of subpopulations and all nodes in a given subpopulation choose among finitely many actions, there always exists a QRE of the activation game [McKelvey and Palfrey, 1995].

Remark 3. The parameter c can alternatively be viewed as an incentive given to infected nodes to self-isolate or self-quarantine themselves. In both interpretations (penalty and incentive), the difference in utility $\Delta u_{d,\mathbf{Y}}(\pi, \bar{e}(k)) = 1 - c$.

We now define the risk factor introduced above, followed by characterizing the equilibrium strategies in the activation game.

3.1 Approximating the infection risk for susceptible nodes

For a node v_i with degree d , a natural choice for the risk factor $\mathbb{R}_d(\pi, \bar{e}(k)|v_i(k) \in \mathbf{SA})$ introduced above is the probability with which the susceptible node becomes infected upon activation, i.e., the quantity $\mathbb{P}(v_i(k+1) \in \mathbf{X}|v_i(k) \in \mathbf{SA}; \pi)$. Computing this probability may be prohibitive in large-scale networks as each node needs to know the epidemic states of every other node. Therefore, we compute an approximate upper bound on this probability in a manner analogous to our derivation of mean-field approximations and define the risk factor in terms of this upper bound. Specifically, when the epidemic state is $e(k)$ and strategy profile of the nodes is π , we have

$$\mathbb{P}(v_i(k+1) \in \mathbf{X}|v_i(k) \in \mathbf{SA}; \pi)$$

$$\begin{aligned}
&= \mathbb{E}\left[1 - \prod_{j \neq i} [1 - A_{ij}(k)(X_j(k)N_{\beta_x} + Y_j(k)N_{\beta_y})] \mid v_i(k) \in \mathbf{SA}; \pi\right] \\
&\leq \mathbb{E}\left[\sum_{j \neq i} [A_{ij}(k)(X_j(k)N_{\beta_x} + Y_j(k)N_{\beta_y})] \mid v_i(k) \in \mathbf{SA}; \pi\right] \\
&= \sum_{j \neq i} \beta_x \mathbb{E}[A_{ij}(k)X_j(k) \mid v_i(k) \in \mathbf{SA}; \pi] + \beta_y \mathbb{E}[A_{ij}(k)Y_j(k) \mid v_i(k) \in \mathbf{SA}; \pi], \tag{16}
\end{aligned}$$

where the inequality is an application of Weierstrass product inequality.

We now compute the above two expectation terms for a node v_j with degree t . Recall from (9) that $\Gamma_{i \rightarrow j}^k$ denotes the event that node v_i activates and forms an edge with node v_j at time k . We denote by \mathbf{SAX}_{ij}^k the event that v_i is susceptible and activates itself while v_j is asymptotically infected at time k . We compute

$$\begin{aligned}
&\mathbb{E}[A_{ij}(k)X_j(k) \mid v_i(k) \in \mathbf{SA}; \pi] \\
&= \mathbb{P}(A_{ij}(k) = 1 \mid v_i(k) \in \mathbf{SA}, X_j(k) = 1; \pi) \mathbb{P}(X_j(k) = 1) \\
&= \left[1 - [1 - \mathbb{P}(\Gamma_{i \rightarrow j}^k \mid \mathbf{SAX}_{ij}^k; \pi)][1 - \mathbb{P}(\Gamma_{j \rightarrow i}^k \mid \mathbf{SAX}_{ij}^k; \pi)]\right] x_t(k) \\
&= [1 - [1 - \bar{d}][1 - \bar{t}\pi_{t,\mathbf{X}}]] x_t(k) \\
&= [\bar{t}\pi_{t,\mathbf{X}} + \bar{d}(1 - \bar{t}\pi_{t,\mathbf{X}})] x_t(k),
\end{aligned}$$

where $\bar{d} = d/(n-1)$ is the probability of node v_i choosing a specific node v_j ; the interpretation of \bar{t} is analogous. Furthermore, $\mathbb{P}(X_j(k) = 1) = x_t(k)$ as node j is chosen at random and $x_t(k)$ denotes the proportion of nodes with degree t that are in state \mathbf{X} at time k . Following identical arguments, we obtain

$$\mathbb{E}[A_{ij}(k)Y_j(k) \mid v_i(k) \in \mathbf{SA}; \pi] = [\bar{t}\pi_{t,\mathbf{Y}} + \bar{d}(1 - \bar{t}\pi_{t,\mathbf{Y}})] y_t(k). \tag{17}$$

Note that both expectations evaluate to an identical quantity for all nodes with a given degree t . Now, substituting the above in (16), we obtain

$$\begin{aligned}
&\mathbb{P}(v_i(k+1) \in \mathbf{X} \mid v_i(k) \in \mathbf{SA}; \pi) \\
&\leq \sum_{t \in \mathcal{D}} nm_t \beta_x x_t(k) [\bar{t}\pi_{t,\mathbf{X}} + \bar{d}(1 - \bar{t}\pi_{t,\mathbf{X}})] + nm_t \beta_y y_t(k) [\bar{t}\pi_{t,\mathbf{Y}} + \bar{d}(1 - \bar{t}\pi_{t,\mathbf{Y}})] \\
&\simeq \sum_{t \in \mathcal{D}} m_t \beta_x x_t(k) [t\pi_{t,\mathbf{X}} + d(1 - \bar{t}\pi_{t,\mathbf{X}})] + m_t \beta_y y_t(k) [t\pi_{t,\mathbf{Y}} + d(1 - \bar{t}\pi_{t,\mathbf{Y}})] \\
&=: \mathbb{R}_d(\pi, \bar{e}(k) \mid v_i(k) \in \mathbf{SA}), \tag{18}
\end{aligned}$$

where the first inequality follows since the number of nodes with degree t is nm_t and the approximate equality follows from $nt/(n-1) \simeq t$ for large values of n . The risk factor thus defined in (18) is a function of the proportion of asymptomatic and symptomatic nodes and the activation probabilities in asymptomatic and symptomatic states for each degree $d \in \mathcal{D}$.

We now follow analogous arguments and approximate the probability of a susceptible node v_i with degree d becoming infected when it does not activate as

$$\begin{aligned}
&\mathbb{P}(v_i(k+1) \in \mathbf{X} \mid v_i(k) \in \mathbf{SN}; \pi) \\
&\leq \sum_{j \neq i} \beta_x \mathbb{E}[A_{ij}(k)X_j(k) \mid v_i(k) \in \mathbf{SN}; \pi] + \beta_y \mathbb{E}[A_{ij}(k)Y_j(k) \mid v_i(k) \in \mathbf{SN}; \pi] \\
&\leq \sum_{t \in \mathcal{D}} nm_t \beta_x \mathbb{P}(A_{ij}(k) = 1 \mid v_i(k) \in \mathbf{SN}, X_j(k) = 1, d_j = t; \pi) \mathbb{P}(X_j(k) = 1 \mid d_j = t)
\end{aligned}$$

$$\begin{aligned}
& + \sum_{t \in \mathcal{D}} nm_t \beta_y \mathbb{P}(A_{ij}(k) = 1 | v_i(k) \in \text{SN}, Y_j(k) = 1, d_j = t; \pi) \mathbb{P}(Y_j(k) = 1 | d_j = t) \\
& = \sum_{t \in \mathcal{D}} nm_t \beta_x x_t(k) \mathbb{P}(\Gamma_{j \rightarrow i}^k | \mathbf{SX}_{ij}^k; \pi) + nm_t \beta_y y_t(k) \mathbb{P}(\Gamma_{j \rightarrow i}^k | \mathbf{SY}_{ij}^k; \pi) \\
& = \sum_{t \in \mathcal{D}} nm_t \beta_x x_t(k) \bar{t} \pi_{t,X} + nm_t \beta_y y_t(k) \bar{t} \pi_{t,Y} \\
& \simeq \sum_{t \in \mathcal{D}} \beta_x m_t x_t(k) t \pi_{t,X} + \beta_y m_t y_t(k) t \pi_{t,Y} =: \mathbb{R}_d(\pi, \bar{e}(k) | v(k) \in \text{SN}). \tag{19}
\end{aligned}$$

We further note from Definition 4 that the equilibrium activation probability is a function of the difference in the utility of the nodes $\Delta u_{d,S}(\pi, \bar{e}(k))$. Therefore, we compute

$$\begin{aligned}
\Delta u_{d,S}(\pi, \bar{e}(k)) & = u_{d,S}(\mathbf{A}, \pi, \bar{e}(k)) - u_{d,S}(\mathbf{N}, \pi, \bar{e}(k)) \\
& = 1 - L[\mathbb{R}_d(\pi, \bar{e}(k) | v(k) \in \text{SA}) - \mathbb{R}_d(\pi, \bar{e}(k) | v(k) \in \text{SN})] \\
& = 1 - L \left[\sum_{t \in \mathcal{D}} m_t \beta_x x_t(k) d(1 - \bar{t} \pi_{t,X}) + m_t \beta_y y_t(k) d(1 - \bar{t} \pi_{t,Y}) \right].
\end{aligned}$$

Thus, in order to decide whether to activate or not in the proposed framework, a node needs to be aware of the activation probabilities of asymptomatic and symptomatic nodes and the proportion of asymptomatic and symptomatic nodes for each degree present in the network. As a result, even when the nodes are aware of the required information, solving for the QRE requires solving for the solution of $|\mathcal{D}|$ coupled nonlinear equations.

In order to reduce the information and computational burden, we approximate

$$\begin{aligned}
\Delta u_{d,S}(\pi, \bar{e}(k)) & \simeq 1 - L \left[\sum_{t \in \mathcal{D}} m_t \beta_x x_t(k) d + m_t \beta_y y_t(k) d \right] \\
& = 1 - Ld[\beta_x \bar{x}(k) + \beta_y \bar{y}(k)], \tag{20}
\end{aligned}$$

which is accurate if the maximum degree $d_{\max} \ll n$ (which implies $1 - \bar{t} \pi_{t,Z} = 1 - t/(n-1)\pi_{t,Z} \simeq 1$). The above expression is also independent of the activation decisions of other nodes. We have defined $\bar{x}(k) := \sum_{t \in \mathcal{D}} m_t x_t(k)$ and $\bar{y}(k) := \sum_{t \in \mathcal{D}} m_t y_t(k)$ as the expected fraction of (all) nodes that are asymptomatic and symptomatic at time k . In the subsequent analysis and in our simulations, we use the approximation in (20) and assume that the nodes are aware of $\bar{e}(k) = (\bar{x}(k), \bar{y}(k))$ at each time k .

3.2 Activation Probabilities at the Quantal Response Equilibrium

The following result characterizes the activation probabilities of the nodes at the QRE in different epidemic states of the A-SAIR model.

Proposition 1. *Consider the A-SAIR epidemic model with the utility functions of the nodes as defined in (14). Let the nodes be aware of $\bar{e}(k) = (\bar{x}(k), \bar{y}(k))$ at time k and let $\Delta u_{d,S}(\pi, \bar{e}(k))$ be given as (20). Then, the activation probabilities of the nodes at the quantal response equilibrium with parameter λ are given by*

$$\pi_{d,S,NE}^\lambda(k) = \pi_{d,X,NE}^\lambda(k) = \frac{e^{\lambda - \lambda Ld[\beta_x \bar{x}(k) + \beta_y \bar{y}(k)]}}{e^{\lambda - \lambda Ld[\beta_x \bar{x}(k) + \beta_y \bar{y}(k)]} + 1}, \tag{21}$$

$$\pi_{d,R,NE}^\lambda(k) = \frac{e^\lambda}{e^\lambda + 1}, \quad \pi_{d,Y,NE}^\lambda(k) = \frac{e^{\lambda(1-c)}}{e^{\lambda(1-c)} + 1}, \quad k \geq 0, d \in \mathcal{D}. \quad \square \tag{22}$$

The above result is a consequence of the fact that the utilities in symptomatic and recovered states do not depend on the node degrees, epidemic states and strategy profile ((14)). Furthermore, in the susceptible and asymptomatic states, the utilities only depend on the node degree and aggregate epidemic states $\bar{x}(k)$ and $\bar{y}(k)$. In other words, the decision problems are essentially decoupled due to the approximations in the previous subsection and the choice of activation probabilities are according to the logit choice model.

The result shows that the nodes use the aggregate epidemic states as *feedback* to determine the equilibrium activation probability $\pi_{d,S,NE}^\lambda(k)$ in a decentralized manner under the logit choice framework. Since nodes with a larger degree experience a greater risk due to exposure to a larger number of nodes, the equilibrium activation probability is monotonically decreasing with respect to the node degree.

When all nodes choose their activation probabilities according to their QRE strategies, the evolution of the epidemic states can be approximated via the DBMF approximation defined in Definition 3 with activation probabilities given by $\pi_{d,Z,NE}^\lambda(k)$, $Z \in \{S, X, Y, R\}$ as stated in Proposition 1.

Remark 4. *We emphasize that though we consider a specific choice of risk factors in this work, other notions of risk/cost of getting infected can be considered in the proposed framework and QRE strategies can be derived following Definition 4.*

We now discuss the implications of Proposition 1 in the A-SIR epidemic model which is a special case of the A-SAIR epidemic model.

3.2.1 A-SIR Epidemic Model

In the conventional SIR epidemic model, there is no distinction between asymptomatic and symptomatic epidemic states. The activity-driven analogue of the SIR epidemic model, denoted by A-SIR epidemic model, is a special case of the A-SAIR epidemic discussed above with the transition rate $\nu = 0$ and $Y_i(0) = 0$ for all nodes v_i . In other words, when none of the nodes are in the symptomatic state and the probability of becoming symptomatic is 0, we recover the A-SIR epidemic model.

The individual-based and degree-based mean-field approximations for the A-SIR model are special cases of the approximations derived in Theorem 1 and Definition 3 with $\nu = 0$ and $y_i(0) = 0$ or $y_d(0) = 0$ for all nodes/degrees.

We now analyze the equilibrium activation probabilities for the A-SIR epidemic model. In this case, we assume that infected nodes are aware of being infected, i.e., they behave as symptomatic nodes in the A-SAIR model. As a consequence of the analysis in the previous subsection and Proposition 1, we have

$$\pi_{d,R,NE}^\lambda(k) = \frac{e^\lambda}{e^\lambda + 1}, \quad \pi_{d,X,NE}^\lambda(k) = \frac{e^{\lambda(1-c)}}{e^{\lambda(1-c)} + 1}, \quad (23)$$

$$\pi_{d,S,NE}^\lambda(k) = \frac{e^{\lambda \Delta u_{d,S}(\pi_{NE}^\lambda(k), \bar{x}(k))}}{e^{\lambda \Delta u_{d,S}(\pi_{NE}^\lambda(k), \bar{x}(k))} + 1}, \quad d \in \mathcal{D}, \quad (24)$$

where

$$\Delta u_{d,S}(\pi_{NE}^\lambda(k), \bar{x}(k)) = 1 - Ld \sum_{t \in \mathcal{D}} \beta_x m_t x_t(k) (1 - t \pi_{t,X,NE}^\lambda) \simeq 1 - Ld \beta_x \bar{x}(k), \quad (25)$$

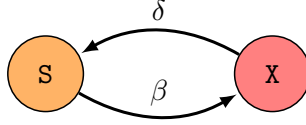


Figure 2: Probabilistic evolution of states in the A-SIS epidemic model. Self-loops are omitted for better clarity. See Definition 5 for the formal definition.

following (20). In the special case when all nodes have an identical degree d , then $\bar{x}(k) = x_d(k)$. When we investigate the evolution of the epidemic states in this special case in Section 5, we consider the activation probabilities given above with

$$\Delta u_{d,S}(\pi_{\text{NE}}^\lambda(k), \bar{x}(k)) = 1 - Ld\beta_x x_d(k)(1 - d\pi_{d,X,\text{NE}}^\lambda). \quad (26)$$

In the following section, we define the activity-driven SIS epidemic model and characterize equilibrium activation probabilities therein. In Section 5, detailed simulations are carried out for both epidemic models under game-theoretic activation and the impacts of cost parameters, λ and degree distribution are investigated.

4 A-SIS Epidemic under Game-Theoretic Activation

We now consider the activity-driven SIS epidemic (A-SIS) model under game-theoretic activation decisions by the nodes. An analogous model was first introduced in [Ogura et al., 2019] with state-dependent activation probabilities, but without any strategic decision-making by the nodes. We now formally define a general version of the model below.

In the A-SIS epidemic model, each node remains in two possible states: susceptible (S) and infected (X). Given a network or contact pattern, the probabilistic state evolution is defined below which is analogous to Definition 1.

Definition 5. *Let $\beta, \delta \in [0, 1]$ be constants pertaining to infection and recovery rates. The state of each node v_i evolves as follows.*

1. *If $v_i(k) \in \mathbf{S}$, then $v_i(k+1) \in \mathbf{X}$ with probability β for each infected neighbor independently of other neighbors.*
2. *If $v_i(k) \in \mathbf{X}$, then $v_i(k+1) \in \mathbf{S}$ with probability δ .*

The state remains unchanged otherwise. □

The state transitions are illustrated in Figure 2. The state-dependent evolution of the network or contact pattern is analogous to the definition in the A-SAIR epidemic setting (Definition 2) with the only distinction being that nodes can be in one of two possible states and the epidemic parameters are β and δ defined above. We denote the activation probabilities of node v_i at time k when it is susceptible and infected by $\pi_{\mathbf{S},i}(k)$ and $\pi_{\mathbf{X},i}(k)$, respectively.

In this section, we first derive the individual-based and degree-based mean-field approximations to the exact Markovian state evolution. We then derive the activation probabilities chosen by the nodes in different states at the QRE, followed by analyzing the closed-loop dynamics.

4.1 State Evolution and Mean-Field Approximations

We follow analogous notations and arguments as the A-SAIR epidemic model from Section 2.1. For a node v_i , we define a random variable $X_i(k)$ to indicate its state at time k with $X_i(k) = 1$ if v_i is infected at time k and $X_i(k) = 0$ if it is susceptible. Under the A-SIS epidemic, the state of v_i evolves as

$$X_i(k+1) = (1 - N_\delta)X_i(k) + (1 - X_i(k)) \left[1 - \prod_{j \neq i} [1 - A_{ij}(k)X_j(k)N_\beta] \right], \quad (27)$$

where $A_{ij}(k)$, N_δ and N_β are as defined in Section 2.1. We define $x_i(k) := \mathbb{P}(X_i(k) = 1) = \mathbb{E}[X_i(k) = 1]$ as before. Note that the epidemic states follow a Markov process with a $2^n \times 2^n$ transition probability matrix. The following result derives an individual-based mean-field approximation. The proof is analogous to the proof of Theorem 1.

Theorem 2. *Consider the A-SIS epidemic model where node v_i upon activation connects to d_i other nodes upon activation. Let $\bar{d}_i = d_i/(n-1)$. Then,*

$$\begin{aligned} x_i(k+1) &\simeq (1 - \delta)x_i(k) + (1 - x_i(k)) \sum_{j \neq i} \beta [1 - (1 - \pi_{\mathbf{S},i}(k)\bar{d}_i)(1 - \pi_{\mathbf{X},j}(k)\bar{d}_j)] x_j(k) \\ &\leq (1 - \delta)x_i(k) + \sum_{j \neq i} \beta [1 - (1 - \pi_{\mathbf{S},i}(k)\bar{d}_i)(1 - \pi_{\mathbf{X},j}(k)\bar{d}_j)] x_j(k), \end{aligned} \quad (28)$$

for all nodes v_i and $k \geq 0$. □

Proof. We compute expectation on both sides of (27) and obtain

$$\begin{aligned} x_i(k+1) &= (1 - \delta)x_i(k) + \mathbb{E} \left[(1 - X_i(k)) \left[1 - \prod_{j \neq i} [1 - A_{ij}(k)X_j(k)N_\beta] \right] \right] \\ &\leq (1 - \delta)x_i(k) + \sum_{j \neq i} \beta \mathbb{E} [A_{ij}(k)X_j(k)(1 - X_i(k))] \end{aligned} \quad (29)$$

$$= (1 - \delta)x_i(k) + \sum_{j \neq i} \beta \mathbb{P}(A_{ij}(k) = 1 | \mathbf{S}_{ij}^k) \mathbb{P}(\mathbf{S}_{ij}^k), \quad (30)$$

following Weierstrass product inequality. Here, \mathbf{S}_{ij}^k denotes the event that node $v_i(k) \in \mathbf{S}$ (i.e., $X_i(k) = 0$) and node $v_j(k) \in \mathbf{X}$ (i.e., $X_j(k) = 1$) as in (7). We now compute

$$\begin{aligned} \mathbb{P}(A_{ij}(k) = 1 | \mathbf{S}_{ij}^k) &= \mathbb{P}(\Gamma_{i \rightarrow j}^k \cup \Gamma_{j \rightarrow i}^k | \mathbf{S}_{ij}^k) \\ &= 1 - [1 - \mathbb{P}(\Gamma_{i \rightarrow j}^k | \mathbf{S}_{ij}^k)][1 - \mathbb{P}(\Gamma_{j \rightarrow i}^k | \mathbf{S}_{ij}^k)] \\ &= 1 - [1 - \pi_{\mathbf{S},i}(k)\bar{d}_i][1 - \pi_{\mathbf{X},j}(k)\bar{d}_j], \end{aligned} \quad (31)$$

where $\Gamma_{i \rightarrow j}^k$ is as defined in (9). Note that the probability of an activated node v_i choosing a specific node v_j is $\bar{d}_i = \frac{d_i}{n-1}$.

We now approximate $\mathbb{P}(\mathbf{S}_{ij}^k) \simeq (1 - x_i(k))x_j(k)$ assuming that states of nodes v_i and v_j are independent. The result now follows upon substituting (31) in (30). The upper bound follows from the fact that $1 - x_i(k) \leq 1$. □

The above theorem shows that the evolution of infection probabilities of the nodes can be upper bounded by a *linear* dynamics. This approximation is analogous to the deterministic evolution and the N-Intertwined Mean-Field Approximation (NIMFA) of the classical SIS epidemic [Van Mieghem, 2011]. We now define the DBMF approximation of the A-SIS epidemic model when all nodes of a given degree choose an identical activation probability.

Definition 6. Consider the A-SIS epidemic model defined in Definition 5. Let all nodes with degree $d \in \mathcal{D}$ choose an identical (state-dependent) activation probability denoted by $\pi_{d,\mathbf{z}}(k)$ with $\mathbf{z} \in \{\mathbf{S}, \mathbf{X}\}$. Then, the proportion of nodes with degree d that are infected evolves as

$$\begin{aligned} x_d(k+1) &= (1-\delta)x_d(k) + (1-x_d(k)) \sum_{t \in \mathcal{D}} nm_t \beta [1 - (1 - \pi_{d,\mathbf{S}}(k)\bar{d})(1 - \pi_{t,\mathbf{X}}(k)\bar{t})] x_t(k) \\ &\leq (1-\delta)x_d(k) + \sum_{t \in \mathcal{D}} nm_t \beta [1 - (1 - \pi_{d,\mathbf{S}}(k)\bar{d})(1 - \pi_{t,\mathbf{X}}(k)\bar{t})] x_t(k), \end{aligned} \quad (32)$$

where $\bar{d} = d/(n-1)$ and $\bar{t} = t/(n-1)$. \square

We arrived at the above definition from the individual based mean-field approximation in Theorem 2, by noting that all nodes with degree t contribute an identical quantity to the summation and the number of nodes with degree t is nm_t . The linearized dynamic can be written in more compact form as

$$x(k+1) \leq [\mathbb{I} - D + \mathcal{B}(k)]x(k) =: \mathcal{F}(k)x(k), \quad (33)$$

where $x(k) = \{x_d(k)\}_{d \in \mathcal{D}} \in \mathbb{R}^{|\mathcal{D}|}$ is the vector of proportion of infected nodes, \mathbb{I} is the identity matrix of dimension $|\mathcal{D}|$, $D = \text{diag}(\delta, \dots, \delta)$, and $\mathcal{B}(k) \in \mathbb{R}^{|\mathcal{D}| \times |\mathcal{D}|}$ with $[\mathcal{B}(k)]_{d,t} = nm_t \beta [1 - (1 - \pi_{d,\mathbf{S}}(k)\bar{d})(1 - \pi_{t,\mathbf{X}}(k)\bar{t})]$.

In the classical networked SIS epidemic on static networks, the infection dynamic under the mean-field approximations (MFAs) exhibits an interesting behavior: if the linearized dynamic is Schur stable, then the infection is eradicated exponentially fast, else there exists a non-zero *endemic equilibrium* of the mean-field dynamic where the infection persists [Mei et al., 2017, Paré et al., 2020b]. We note that the MFAs of the A-SIS epidemic have an analogous structure as the classical SIS epidemic. If the activation probabilities remain constant as the epidemic evolves, then we have the following result on their equilibrium behavior which follows from [Paré et al., 2020b, Theorem 1, 2].

Proposition 2. Consider the DBMF approximation of the A-SIS epidemic in Definition 6 with $\delta, \beta \in [0, 1]$. Let the activation probabilities be positive, static and denoted by $\pi_{d,\mathbf{S}}, \pi_{d,\mathbf{X}}$ for $d \in \mathcal{D}$. Let $\beta(d_{\text{avg}} + d_{\text{max}}) \leq 1$ and the matrix $\mathcal{F} \in \mathbb{R}^{|\mathcal{D}| \times |\mathcal{D}|}$ have entries

$$[\mathcal{F}]_{d,t} = \begin{cases} (1-\delta) + nm_d \beta [1 - (1 - \pi_{d,\mathbf{S}}\bar{d})(1 - \pi_{d,\mathbf{X}}\bar{d})], & \text{if } t = d, \\ nm_t \beta [1 - (1 - \pi_{d,\mathbf{S}}\bar{d})(1 - \pi_{t,\mathbf{X}}\bar{t})], & \text{otherwise.} \end{cases}$$

Let $\rho(\mathcal{F})$ denote the spectral radius of \mathcal{F} . Then,

1. If $\rho(\mathcal{F}) \leq 1$, then $x = 0$ is the unique equilibrium of (32) which is asymptotically stable with domain of attraction $[0, 1]^{|\mathcal{D}|}$, and
2. if $\rho(\mathcal{F}) > 1$, there is an additional equilibrium x^* of (32) with $x^*(d) > 0, \forall d \in \mathcal{D}$.

Proof. The result follows from [Paré et al., 2020b, Theorem 1, 2] which holds under Assumptions 1-5 stated in [Paré et al., 2020b]. Since $\delta, \beta \in [0, 1]$ and $\pi_{d,\mathbf{S}} > 0, \pi_{d,\mathbf{X}} > 0$, Assumptions 1,2, 4 and 5 are satisfied. It only remains to show that $\sum_{t \neq d} [\mathcal{B}]_{d,t} \leq 1$ for all $d \in \mathcal{D}$ (Assumption 3 in [Paré et al., 2020b]). For a given degree $d \in \mathcal{D}$, we compute

$$\sum_{t \neq d} [\mathcal{B}]_{d,t} \leq \sum_{t \in \mathcal{D}} nm_t \beta [1 - (1 - \pi_{d,\mathbf{S}}\bar{d})(1 - \pi_{t,\mathbf{X}}\bar{t})]$$

$$\begin{aligned}
&\leq \sum_{t \in \mathcal{D}} nm_t \beta [\pi_{d,S} \bar{d} + \pi_{t,X} \bar{t}] \\
&\leq \sum_{t \in \mathcal{D}} nm_t \beta (\bar{d} + \bar{t}) \simeq \sum_{t \in \mathcal{D}} (m_t \beta d + m_t \beta t) = \beta (d + d_{\text{avg}}),
\end{aligned}$$

where we assume $n \simeq n - 1$ (which is accurate when the number of nodes is sufficiently large) and $\pi_{d,S} \leq 1, \pi_{t,X} \leq 1$ being probabilities. Thus, when $\beta (d_{\text{avg}} + d_{\text{max}}) \leq 1$, Assumption 3 in [Paré et al., 2020b] is also satisfied. This concludes the proof. \square

While we have stated the above result for the DBMF approximation, an analogous result holds for the individual-based MFA derived in Theorem 2 as well. We omit the details in the interest of space.

Remark 5. Note that the model in [Ogura et al., 2019] assumes that all nodes have homogeneous degrees and the probability of forming an edge to an infected node is potentially smaller than 1. In a recent prior work [Hota and Gupta, 2020], we identified and corrected an inaccuracy pertaining to the characterization of the quantity $\rho(\mathcal{F})$ in [Ogura et al., 2019].

4.2 Game-Theoretic Choice of Activation Probabilities

We now consider the activation game for the SIS epidemic model. Analogous to the setting studied for the A-SAIR epidemic in Section 3, we assume that all nodes with a given degree d choose an identical activation probability. We now formally define the utilities of the nodes building upon the setting in Section 3.

We assume that all nodes receive benefit 1 upon activation. However, an infected node incurs a cost $c \in \mathbb{R}_+$ if it activates. Susceptible nodes weight the risk of becoming infected in the next time step by a loss $L \in \mathbb{R}_+$. Formally, let $\pi_{d,Z} \in [0, 1]$ denotes the activation probability of a node with degree d in epidemic state $Z \in \{\mathbf{S}, \mathbf{X}\}$. The strategy profile of the nodes is denoted by $\pi := \{\pi_{d,S}, \pi_{d,X}\}_{d \in \mathcal{D}} \subseteq [0, 1]^{2|\mathcal{D}|}$. The global epidemic state at time k is denoted by $e(k) := \{x_d(k)\}_{d \in \mathcal{D}}$, i.e, the proportion of infected nodes in each subpopulation. Note that since there are only two epidemic states, we have $s_d(k) = 1 - x_d(k)$. Let $\bar{e}(k)$ denote the information available to the nodes regarding the epidemic state. The utilities of a node v with degree $d \in \mathcal{D}$ in different epidemic states at time k are defined as:

$$u_{d,S}(\mathbf{A}, \pi, \bar{e}(k)) = 1 - L \mathbb{R}_d(\pi, \bar{e}(k) | v(k) \in \mathbf{SA}), \quad (34a)$$

$$u_{d,S}(\mathbf{N}, \pi, \bar{e}(k)) = -L \mathbb{R}_d(\pi, \bar{e}(k) | v(k) \in \mathbf{SN}), \quad (34b)$$

$$u_{d,X}(\mathbf{A}, \pi, \bar{e}(k)) = 1 - c, \quad u_{d,X}(\mathbf{N}, \pi, \bar{e}(k)) = 0, \quad (34c)$$

where $\mathbb{R}_d(\pi, \bar{e}(k) | v(k) \in \mathbf{SA})$ and $\mathbb{R}_d(\pi, \bar{e}(k) | v(k) \in \mathbf{SN})$ denote the respective risk factors for a susceptible node of degree d under strategy profile π if it activates (denoted by \mathbf{SA}) and does not activate (denoted by \mathbf{SN}).

We define the risk factors as approximations of the probability with which a susceptible node becomes infected in the next time step following the approach in Section 3.1. We specifically note that the analysis in Section 3.1 continues to hold for the A-SIS epidemic model when we exclude the symptomatically infected state. Therefore, building upon (18) and (19), we define

$$\begin{aligned}
\mathbb{R}_d(\pi, \bar{e}(k) | v(k) \in \mathbf{SA}) &:= \sum_{t \in \mathcal{D}} \beta m_t x_t(k) [t \pi_{t,X} + d(1 - \bar{t} \pi_{t,X})], \\
\mathbb{R}_d(\pi, \bar{e}(k) | v(k) \in \mathbf{SN}) &:= \sum_{t \in \mathcal{D}} \beta m_t x_t(k) t \pi_{t,X},
\end{aligned}$$

$$\begin{aligned}\Delta u_{d,S}(\pi, \bar{e}(k)) &= 1 - L \left[\sum_{t \in \mathcal{D}} m_t \beta x_t(k) d (1 - \bar{t} \pi_{t,X}) \right] \\ &\simeq 1 - L \left[\sum_{t \in \mathcal{D}} m_t \beta x_t(k) d \right] = 1 - L d \beta \bar{x}(k),\end{aligned}$$

where $\bar{x}(k)$ is the proportion of nodes that are infected at time k (across all subpopulations) and we have assumed $d_{\max} \ll n$. Accordingly, the activation probabilities at the QRE with parameter λ are given by

$$\pi_{d,S,NE}^\lambda(k) = \frac{e^{\lambda - \lambda L d \beta \bar{x}(k)}}{e^{\lambda - \lambda L d \beta \bar{x}(k)} + 1}, \quad \pi_{d,X,NE}^\lambda(k) = \frac{e^{\lambda(1-c)}}{e^{\lambda(1-c)} + 1} =: \pi_c^\lambda, \quad d \in \mathcal{D}. \quad (35)$$

In other words, nodes use the information regarding the proportion of infected nodes in the network as feedback and adjust their the activation probabilities to maximize their individual utility in the logistic quantal response choice model. When $\lambda = 0$, the activation probabilities are 0.5. For larger values of λ , nodes choose the action that leads to a higher utility with a greater probability.

When a node is already infected, the activation decision depends on the penalty parameter c . When $c > 1$, the penalty is larger than the benefit from activation, and as a result, $\pi_c^\lambda \rightarrow 0$ as $\lambda \rightarrow \infty$. For susceptible nodes, the higher the degree and the prevalence of the epidemic, the smaller is the activation probability at the QRE. For sufficiently high λ , if $dL\beta\bar{x}(k) < 1$, then nodes activate with high probability; otherwise the equilibrium activation probability is negligible. The above model captures the activation decisions made by humans in the midst of the epidemic in a manner that is mathematically rigorous and grounded in behavioral choice models.

4.3 Analysis of Closed-Loop Dynamics

We now analyze the evolution of the epidemic states when nodes choose their activation probabilities according to (35) in the DBMF approximation framework. Let $\delta^c = 1 - \delta$. Following Definition 6, the evolution of the proportion of infected nodes with degree d is given by

$$\begin{aligned}x_d(k+1) &= \delta^c x_d(k) + (1 - x_d(k)) \sum_{t \in \mathcal{D}} n m_t \beta [1 - (1 - \pi_{d,S,NE}^\lambda(k) \bar{d})(1 - \pi_{t,X,NE}^\lambda(k) \bar{t})] x_t(k) \\ &\leq \delta^c x_d(k) + (1 - x_d(k)) \sum_{t \in \mathcal{D}} n m_t \beta [\pi_{d,S,NE}^\lambda(k) \bar{d} + \pi_{t,X,NE}^\lambda(k) \bar{t}] x_t(k) \\ &\simeq \delta^c x_d(k) + (1 - x_d(k)) \sum_{t \in \mathcal{D}} \beta m_t [\pi_{d,S,NE}^\lambda(k) d + \pi_{t,X,NE}^\lambda(k) t] x_t(k) \\ &= \delta^c x_d(k) + (1 - x_d(k)) \sum_{t \in \mathcal{D}} \beta m_t \left[d \frac{e^{\lambda - \lambda L d \beta \bar{x}(k)}}{e^{\lambda - \lambda L d \beta \bar{x}(k)} + 1} + \pi_c^\lambda t \right] x_t(k).\end{aligned} \quad (36)$$

Note that under QRE activation probabilities, the upper bound on $x_d(k+1)$ is nonlinear as $\pi_{d,S,NE}^\lambda(k)$ depends on $\bar{x}(k)$. Therefore, the equilibrium characterization from Proposition 2 is not applicable here. We now exploit the structure of (36) to obtain further insights on the characteristic of the closed-loop dynamic for specific parameter regimes.

Case 1: $\lambda = 0$. In this case, the nodes choose the activation probability to be 0.5 irrespective of their degree and epidemic state. Therefore, we have

$$x_d(k+1) \leq \delta^c x_d(k) + (1 - x_d(k)) \sum_{t \in \mathcal{D}} \beta m_t \frac{d+t}{2} x_t(k). \quad (37)$$

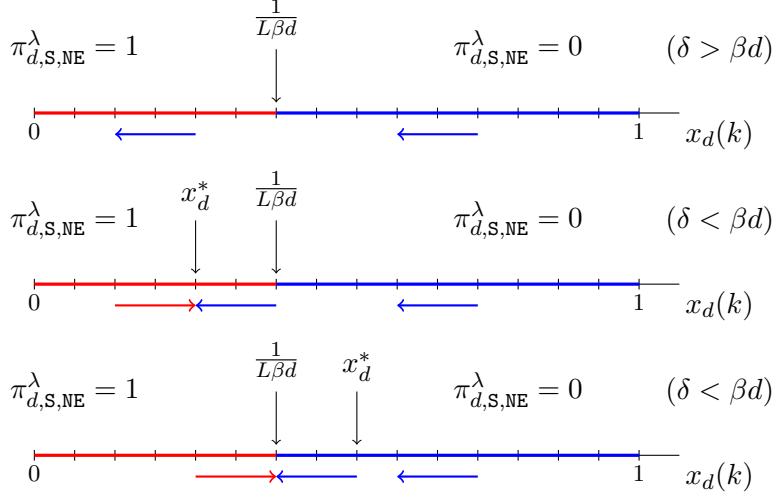


Figure 3: Epidemic evolution when $\lambda \rightarrow \infty, c = 1, m_d = 1$ (Case 3). The arrows indicate the direction along which $x_d(k)$ evolves.

In this case, it follows from Proposition 2 that the proportion of infected nodes decays to 0 exponentially fast if the spectral radius $\rho(\mathcal{F}^0) < 1$, where

$$[\mathcal{F}^0]_{d,t} = \begin{cases} (1 - \delta) + \beta m_d d, & \text{if } t = d \\ \beta m_t \frac{d+t}{2}, & \text{otherwise.} \end{cases}$$

In this case, the condition for epidemic eradication is independent of cost parameters (c and L) as the activation decisions are not strategic.

Case 2: $\lambda \rightarrow \infty, c > 1$. In this regime, the cost of activation exceeds the benefit for infected nodes, and therefore, $\pi_c^\lambda \rightarrow 0$ as $\lambda \rightarrow \infty$. Consequently, from (36), we have

$$\begin{aligned} x_d(k+1) &\leq \delta^c x_d(k) + (1 - x_d(k)) \sum_{t \in \mathcal{D}} \beta m_t \left[d \frac{e^{\lambda - \lambda L d \beta \bar{x}(k)}}{e^{\lambda - \lambda L d \beta \bar{x}(k)} + 1} \right] x_t(k) \\ &\leq \delta^c x_d(k) + \beta d \bar{x}(k) \frac{e^{\lambda - \lambda L d \beta \bar{x}(k)}}{e^{\lambda - \lambda L d \beta \bar{x}(k)} + 1} \leq \delta^c x_d(k) + \beta d \bar{x}(k), \\ \implies \sum_{t \in \mathcal{D}} m_t x_t(k+1) &\leq \delta^c \sum_{t \in \mathcal{D}} m_t x_t(k) + \beta \bar{x}(k) \sum_{t \in \mathcal{D}} m_t t \\ \implies \bar{x}(k+1) &\leq \delta^c \bar{x}(k) + \beta d_{\text{avg}} \bar{x}(k). \end{aligned}$$

Therefore, the epidemic is eradicated when $\delta > \beta d_{\text{avg}}$ in this regime. In the above analysis, we have used the inequality $\pi_{d,S,NE}^\lambda \leq 1$ which is not very tight. In fact, if $\beta d L \bar{x}(k)$ is large, then $\pi_{d,S,NE}^\lambda$ is approximately 0. We now exploit the structure of $\pi_{d,S,NE}^\lambda$ when all nodes have degree d .

Case 3: $\lambda \rightarrow \infty, c > 1, m_d = 1$ (**homogeneous degree**). When all nodes have degree d , i.e., $m_d = 1$, then (36) yields

$$x_d(k+1) = \delta^c x_d(k) + (1 - x_d(k)) \beta d x_d(k) \left[\frac{e^{\lambda - \lambda L d \beta x_d(k)}}{e^{\lambda - \lambda L d \beta x_d(k)} + 1} + \pi_c^\lambda \right].$$

When $c > 1$ and $\lambda \rightarrow \infty$, we have $\pi_c^\lambda \rightarrow 0$. Consequently, we have

$$x_d(k+1) = \begin{cases} \delta^c x_d(k), & \text{if } x_d(k) \in (\frac{1}{L\beta d}, 1], \\ \delta^c x_d(k) + (1 - x_d(k))\beta d x_d(k), & \text{if } x_d(k) \in [0, \frac{1}{L\beta d}) \\ \delta^c x_d(k) + (1 - x_d(k))\beta d x_d(k)\frac{1}{2}, & \text{if } x_d(k) = \frac{1}{L\beta d}. \end{cases}$$

The above dynamic has the following characteristics.

- When the proportion of infected nodes $x_d(k)$ exceeds $\frac{1}{L\beta d}$, susceptible nodes stop activating and as a result, $x_d(k)$ declines at rate δ .
- If $x_d(k) < \frac{1}{L\beta d}$, infected nodes activate with probability 1 as $\lambda \rightarrow \infty$. If the curing rate is sufficiently high, i.e., $\delta > \beta d$, then 0 is the only equilibrium point and $x(k+1)$ declines to 0, albeit with rate $\delta - \beta d$.
- If $\delta < \beta d$, there exists an endemic state of the dynamic with $x_d^* = 1 - \frac{\delta}{\beta d}$.
 - If $x_d^* < \frac{1}{L\beta d}$, then we expect $x_d(k)$ to converge to x_d^* .
 - In contrast, if $x_d^* > \frac{1}{L\beta d}$, we expect $x_d(k)$ to oscillate around $\frac{1}{L\beta d}$.

In particular, if $x_d(k) < \frac{1}{L\beta d}$, the infected proportion grows while if $x_d(k) > \frac{1}{L\beta d}$, it declines as susceptible nodes do not activate.

Therefore, by increasing L , the infected proportion can be stabilized at $\frac{1}{L\beta d}$ which can be made arbitrarily small; even in settings where there is an endemic state at $x_d^* > \frac{1}{L\beta d}$. The different sub-cases discussed above are shown in Figure 3.

We numerically illustrate our theoretical findings in the following section.

5 Simulation Results

In this section, we illustrate the evolution of the epidemic states under game-theoretic activation via extensive simulations.

5.1 A-SIR epidemic with homogeneous node degrees

In order to isolate the impacts of game-theoretic activation decisions and cost parameters (λ , c and L) from the impacts of asymptomatic carriers and heterogeneous node degrees, we first consider the special case of A-SIR epidemic with homogeneous node degrees.

We consider a set of $n = 100$ nodes and set the rate of infection $\beta = 0.3$, rate of recovery $\delta = 0.15$ and degree $d = 5$ for all the nodes. We assume that at $k = 0$, 10 nodes are infected and the remaining are susceptible and simulate the evolution of the epidemic states from $k = 0$ to $k = 80$ when the activation probabilities of the nodes are given by the QRE characterization in (23). In Figure 4, we plot the proportion of nodes in infected (X) and recovered (R) states (both actual proportions averaged over 75 independent runs and under the DBMF approximation) and the evolution of the state-dependent activation probabilities for different values of c , L and λ . The proportions under the DBMF approximation closely tracks the actual proportion of nodes in different epidemic states in all cases.

From the figures in the left panel of Figure 4, we observe that if $\lambda = 0$, the activation probability is constant at 0.5 for all nodes irrespective of their epidemic states. This corresponds to the setting

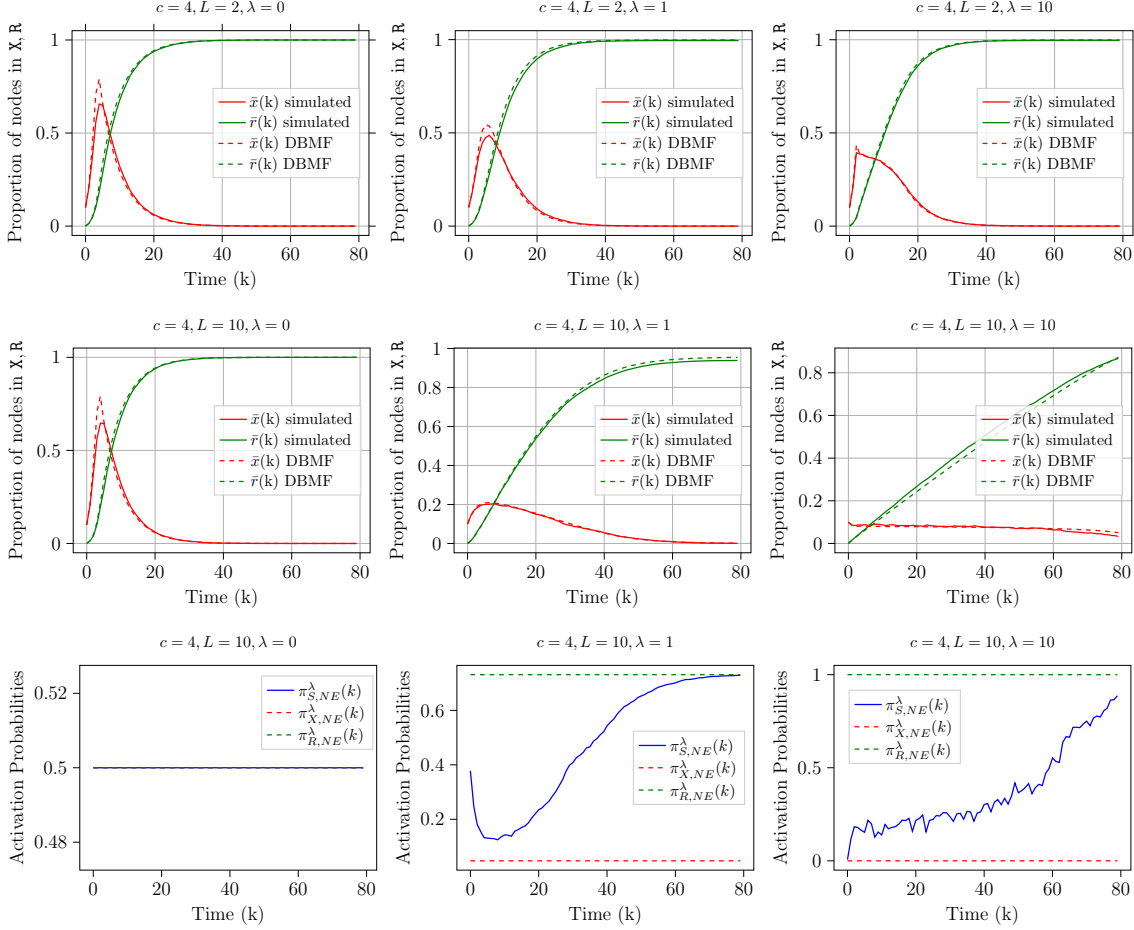


Figure 4: Evolution of the proportion of nodes in infected (X) and recovered (R) states (both actual proportions averaged over 75 independent runs and under the DBMF approximation) and the evolution of the state-dependent activation probabilities at the QRE in the A-SIR epidemic model.

where nodes act completely randomly (independent of the utility they may obtain by activating or not activating). Thus, the state evolution is independent of parameters c and L . In this case, there is a sharp initial increase in the proportion of infected nodes and almost all nodes recover by $k = 40$.

As λ increases, nodes are increasingly likely to take actions that give a higher utility. Nodes that have recovered receive a higher utility upon activation and consequently, the activation probability for recovered nodes is approximately 1 when $\lambda = 10$. The equilibrium activation probability of infected nodes depends on the parameter c which captures the penalty or cost of activation when a node is infected (or incentives offered to self-isolate). When $c > 1$, the activation probability is approximately 0 when λ is sufficiently high. The plots in the bottom row of Figure 4 illustrate this.

The activation probabilities of susceptible nodes at the QRE depend on the proportion of infected nodes (\bar{x}) and is illustrated in Figure 5 for different values of λ and L . We observe the following characteristic from Figure 5:

- as \bar{x} increases, susceptible nodes encounter a larger risk of becoming infected when they activate, and consequently choose a smaller activation probability,
- when the magnitude of loss L is larger, nodes prefer to not activate even when \bar{x} is low to

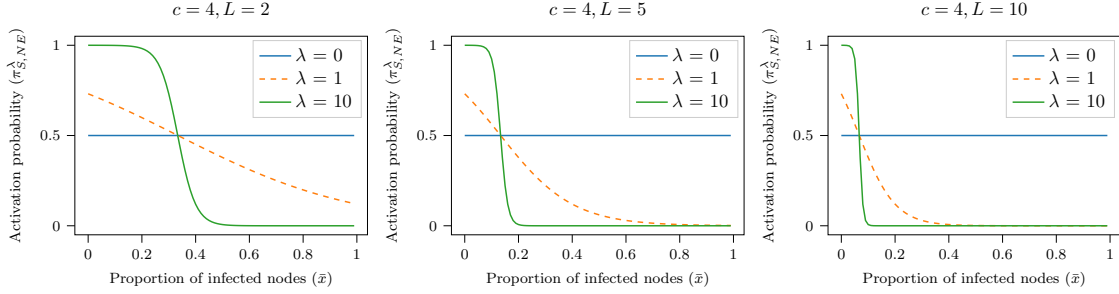


Figure 5: Activation probability for susceptible nodes at the QRE as a function of proportion of infected nodes for different values of λ and L

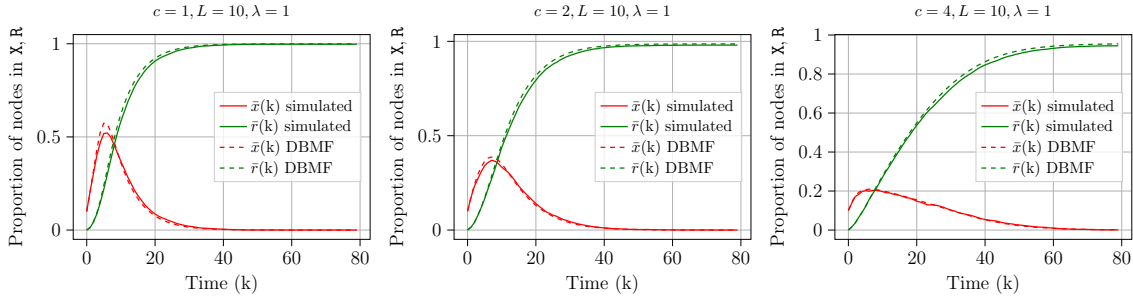


Figure 6: Evolution of the proportion of infected and recovered nodes via simulations and under the DBMF approximation for different values of c .

moderate, and

- when λ is large, there is sharp transition in equilibrium activation probability around the value of \bar{x} at which the nodes are indifferent between activating or not activating (i.e., around \bar{x} where $\Delta u_{d,S}(\pi_{NE}^\lambda, \bar{x}) = 0$).

The above characteristics impact the evolution of epidemic states as shown in Figure 4. The plots in the top row show the evolution for $c = 4$ and $L = 2$ which corresponds to the plot in the left panel of Figure 5. As the proportion of infected nodes exceeds 0.4, the activation probability of susceptible nodes decreases to 0, and consequently, the epidemic dies down. When $\lambda = 10$, the activation probability drops sharply which is reflected in the sharp decline in the proportion of nodes in state X .

When $c = 4$ and $L = 10$, the evolution of states and the activation probability with time is shown in the middle and bottom rows of Figure 4. Note from the plot on the right panel of Figure 5 that the transition in activation probability occurs around the threshold $\bar{x} = 0.1$. Specifically, when $\bar{x}(k)$ is slightly larger than the threshold, the susceptible nodes reduce their activation probabilities. However, this reduction results in $\bar{x}(k)$ decreasing below the threshold which then leads to susceptible nodes increasing their activation probabilities. **As a result, the proportion of nodes in state X fluctuates around the threshold value for a significant amount of time; any reduction in infected proportion is counteracted by an increase in activation probabilities by self-interested nodes.** The plots in the right most panel in the middle and bottom rows in Figure 4 clearly illustrate the above phenomenon. Thus, activation decisions made by self-interested nodes can lead to a *flattening* of the proportion of infected nodes with a much smaller peak but a longer persistence of the infection.

The evolution of the epidemic states for different values of c is shown in Figure 6. The plots show that for larger values of c , the activation probability for infected nodes decreases, and as a result fewer nodes become infected. Thus, the proposed model gives valuable insights to policy-makers on how to set the level of penalty (or incentives) for infected nodes if they violate (adhere to) self-quarantine rules.

5.2 A-SAIR epidemic

In the previous subsection, we examined the impacts of cost parameters c and L and the logistic choice parameter λ on the evolution of epidemic states in the A-SIR epidemic model. We now study the A-SAIR epidemic model. The implications of parameters c , L and λ remain qualitatively unchanged in the A-SAIR epidemic model. Consequently, we focus on understanding the impacts of asymptomatic carriers and heterogeneous node degrees in this subsection.

5.2.1 A-SAIR epidemic with homogeneous node degrees

We consider a set of $n = 100$ nodes and set the infection rates $\beta_x = \beta_y = 0.1$, recovery rate $\delta_y = 0.04$ and degree $d = 5$ for all the nodes. In addition, we choose $\lambda = 10$, $c = 2$, $L = 5$. Figure 7 shows the evolution of proportion of nodes in states X, Y and R and the activation probabilities at the QRE (from Proposition 1) for different values of δ_x and ν . In order to examine the impacts of asymptomatic carriers on epidemic evolution, we consider a variant where nodes are not aware of the proportion of asymptomatic nodes, i.e., they choose the activation probabilities by setting $\bar{x}(k) = 0$. The evolution of the epidemic states in this case are shown in the middle row of Figure 7. The corresponding activation probabilities are shown in the bottom row of Figure 7.

We plot the evolution of states under the DBMF approximation and by taking the average of epidemic states across 50 independent simulations of the activity-driven epidemic model. The figures show that the DBMF approximation is largely accurate.

As shown in the plots in the top row of Figure 7, when the transition rate $\nu = 0.01$, asymptomatic nodes rarely become symptomatic, and largely recover without ever exhibiting symptoms. If the nodes are not aware of the proportion of symptomatic nodes, they continue to activate with probability close to 1. As a result, there is a much larger peak in the asymptomatic proportion (as shown in the plot in the left panel of the middle row) compared to the case when nodes are aware of $\bar{x}(k)$ and reduce their activation probabilities.

In contrast, when $\nu = 0.9$, asymptomatic nodes quickly transition to the symptomatic state. In this case, nodes not being aware of $\bar{x}(k)$ has a more benign effect since most of the infected nodes are symptomatic. When the recovery rate for asymptomatic nodes is higher (i.e., $\delta_x = 0.16$), the epidemic dies quickly as expected.

5.2.2 A-SAIR epidemic with heterogeneous node degrees

We now investigate the evolution of the A-SAIR epidemic in its full generality under game-theoretic activation. We consider a set of $n = 100$ nodes and set $\beta_x = \beta_y = 0.25$, $\delta_x = 0.02$, $\delta_y = 0.1$ and transition rate $\nu = 0.05$. We set the logistic choice parameter $\lambda = 4$ and the loss parameters $L = 4$ and $c = 2$. We compare the epidemic evolution when all nodes have degree 5 (the homogeneous case) with settings where node degrees have a Binomial distribution and a Power-law distribution with exponent 2. The above distributions characterize the degree distributions in several important classes of random graphs [Newman, 2010]. We choose the parameters of these two distributions with $d_{\max} = 20$ such that mean degree approximately 5. Figure 8 shows the results obtained with the above parameters with the respective degree distributions shown in the top panel.

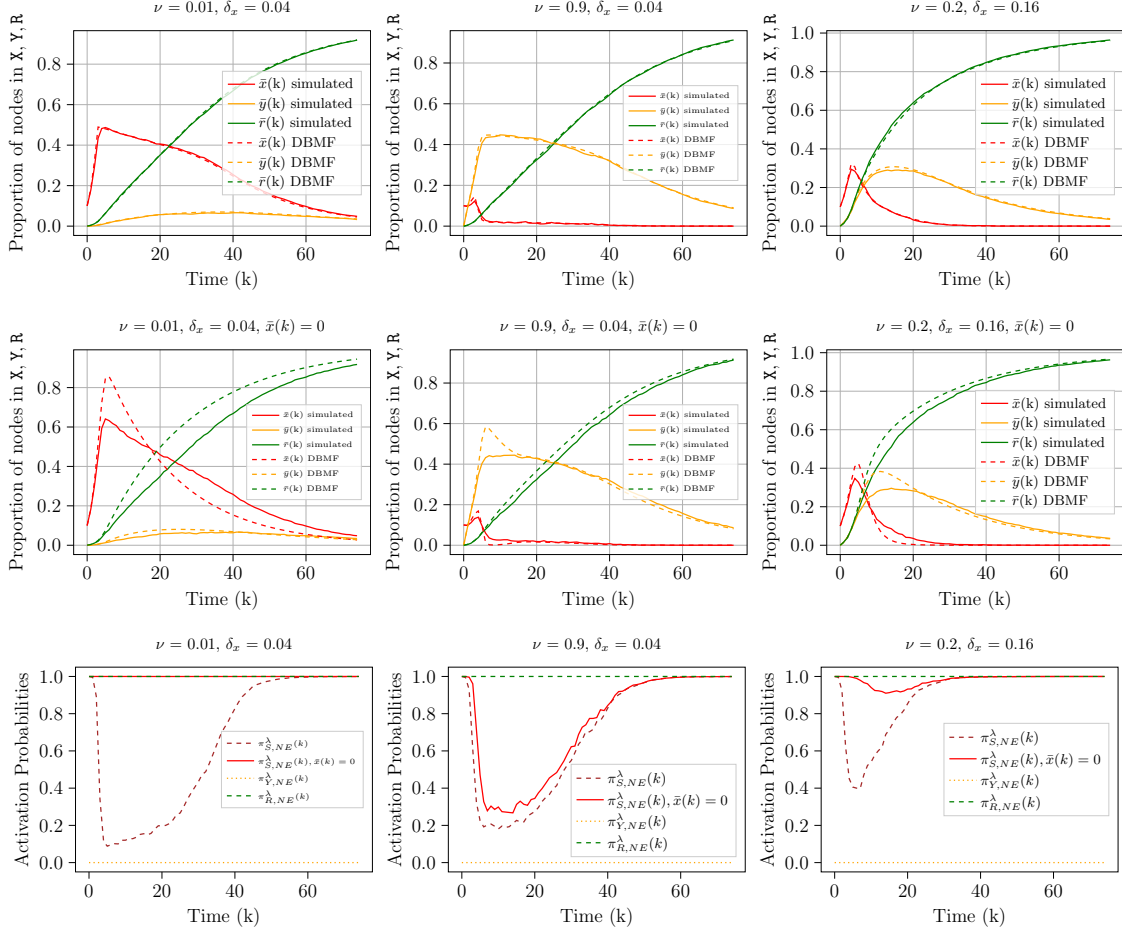


Figure 7: Evolution of the proportion of nodes in asymptomatic (X), symptomatic (Y) and recovered (R) states (both actual proportions averaged over 50 independent runs and under the DBMF approximation) and the evolution of the state-dependent activation probabilities at the QRE in the A-SAIR epidemic model. When nodes take activation decisions without being aware of the proportion of asymptomatic nodes, we denote it by $\bar{x}(k) = 0$.

In the left-most figure on the top panel of Figure 8, we plot the activation probability chosen by susceptible nodes as a function of the proportion of infected nodes ($\bar{x} + \bar{y}$) according to Proposition 1. The plot shows that as $\bar{x} + \bar{y}$ increases, the activation probability decreases for all degrees. We also observe that when d is small, the decline is minimal even when almost all the nodes in the network are infected while for nodes with $d = d_{\max} = 20$, the activation probability drops to 0 when $\bar{x} + \bar{y}$ exceeds 0.2. This confirms our intuition that high degree nodes encounter a larger risk of infection upon activation and as a result, decreases their activity level when the epidemic is prevalent.

The evolution of the proportion of nodes in asymptomatic (X), symptomatic (Y) and recovered (R) states (both actual proportions averaged over 50 independent runs and under the DBMF approximation) and the evolution of the state-dependent activation probabilities at the QRE with time are shown in the middle and bottom panels of Figure 8. Under the chosen parameters, recovered nodes activate with probability approximately 1 and symptomatic nodes activate with probability close to 0.

When all nodes have homogeneous degrees (figures in the left panel), an initial increase in the

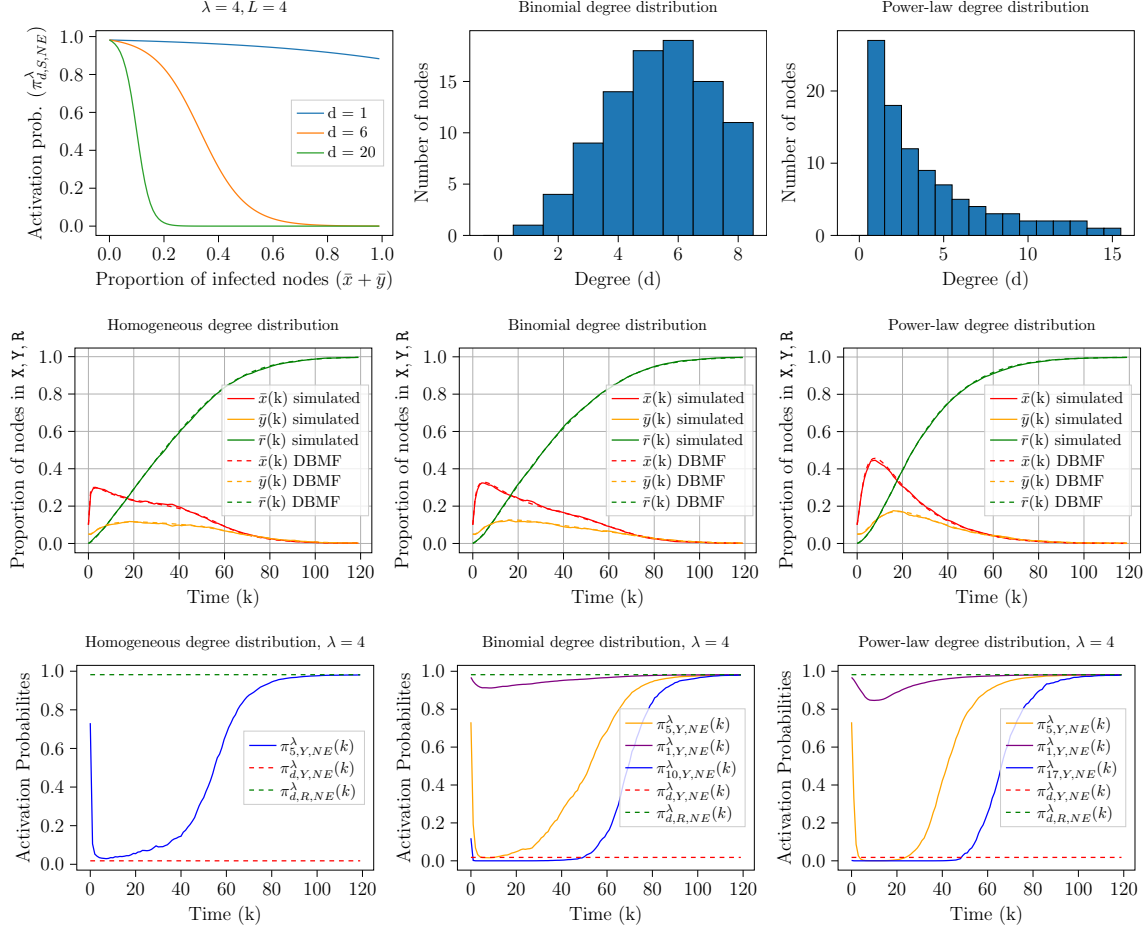


Figure 8: Degree distributions, evolution of the proportion of nodes in asymptomatic (X), symptomatic (Y) and recovered (R) states (both actual proportions averaged over 50 independent runs and under the DBMF approximation) and the evolution of the state-dependent activation probabilities at the QRE in the A-SAIR epidemic model.

infected proportion causes the activation probability of susceptible nodes to fall close to 0 and eventually the epidemic declines. Under the Binomial distribution (middle panel), the activation probabilities depend on the degree of the nodes as well. Specifically, nodes with small degrees continue to activate at a very high rate which leads to a larger peak in the infected proportion compared to the homogeneous case. Under the Power-law degree distribution (right panel), a significant proportion of the nodes have very small degree, and as a result, a large proportion of nodes continue to activate at a high rate leading to an even sharper peak in the infected proportion.

5.3 A-SIS Epidemic

We now examine the evolution of the A-SIS epidemic under game-theoretic activation. We consider $n = 100$ nodes and set the infection rate $\beta = 0.2$, recovery rate $\delta = 0.4$, penalty parameter $c = 10$ and $\lambda = 20$. The evolution of the proportion of infected nodes, both in actual simulations and under the DBMF approximation, for different values of L is shown in Figure 9. The top panel shows the evolution when all nodes have degree 4, and the bottom panel when nodes have a Power-law degree distribution with $d_{\text{avg}} = 4, d_{\text{max}} = 20$ and $\alpha = 2$.

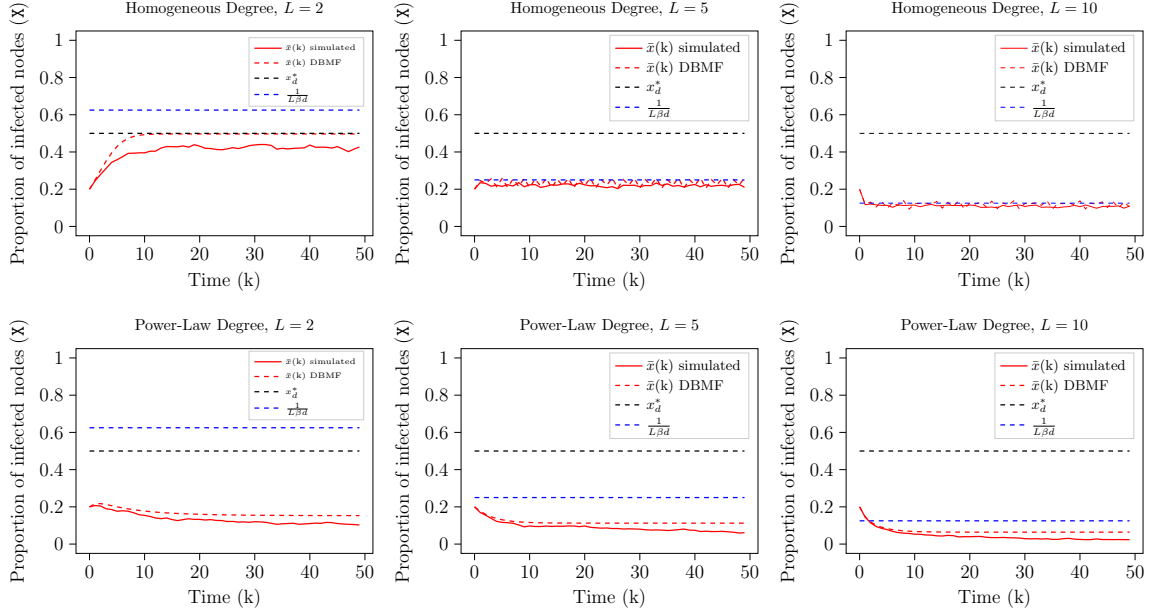


Figure 9: Evolution of the proportion of infected nodes (both actual proportions averaged over 50 independent runs and under the DBMF approximation) in the A-SIS epidemic model.

The plots in the top panel illustrate the theoretical findings discussed in Section 4.3, Case 3. Specifically, for the considered parameters, there exists an endemic state of the epidemic with $x_d^* = 1 - \frac{\delta}{\beta d} = 0.5$. When the loss parameter $L = 2$, the threshold $\frac{1}{L\beta d} = 0.625 > x_d^*$. Accordingly, the infected proportion under the DBMF approximation settles around x_d^* and infected proportion under actual simulation settles at a slightly smaller value. When $L = 5$, we have $\frac{1}{L\beta d} = 0.25 < x_d^*$. We observe that the actual infected fraction and the DBMF approximation oscillates around $\frac{1}{L\beta d}$ as discussed in Section 4.3. Any increase in $x(k)$ beyond $\frac{1}{L\beta d}$ results in activation probability dropping to 0 which causes $x(k)$ to drop down to $\frac{1}{L\beta d}$. Finally, when $L = 10$, the threshold $\frac{1}{L\beta d} = 0.125$. The infected proportion decreases from the initial value of 0.2 to the threshold value. Thus, for sufficiently large L , the infected proportion under game-theoretic activation is considerably smaller than x_d^* .

The plots in the bottom panel of Figure 9 show the evolution under power-law degree distribution for different values of L . In this case, the proportion of infected nodes is smaller than the corresponding results for homogeneous degree distributions under both actual simulations and the DBMF approximation.

6 Discussion and Conclusion

Our work is one of the first to conduct a rigorous and comprehensive analysis of the impacts of game-theoretic activation on epidemic spread over dynamical networks. One of the main insights from our results is that, in both A-SAIR and A-SIS epidemic models, the infection can persist in the population for a long time under game-theoretic activation as any increase and decrease in infected proportion is counteracted by a decrease and increase in the activation probabilities, respectively. We also highlighted the impacts of asymptomatic carriers, heterogeneous degree distributions and bounded rationality in detail. There are several promising directions for future research.

- The analysis of closed-loop dynamics under game-theoretic activation for the SAIR epidemic remains a challenging open problem.
- In our analysis, we show that the equilibrium activation probabilities depend on the proportion of infected nodes. However, this information may not be available in practice as testing data is often not accurate and represents the epidemic state with a certain delay. Therefore, the impacts of inaccurate and delayed information on activation probabilities and epidemic evolution should be investigated.
- In this work, we have assumed that edges or connections are formed with probability 1. This assumption can potentially be relaxed by letting nodes choose whether to accept incoming connections or not in a strategic manner.
- Much of the earlier work on inferring epidemic states and resource allocation for epidemic containment rely on centralized algorithms (e.g., modifying infection and recovery rates) and do not include behavioral changes in the activation pattern of the nodes [Agrawal et al., 2020, Hota et al., 2020, Nowzari et al., 2016]. The analysis carried out in our work should be integrated with inference, estimation and optimal resource allocation schemes to obtain more accurate results.
- Finally, the theoretical predictions should be compared with the mobility data made available for various activities [Google, 2020] from which various parameters of interest (such as λ, L, c) could be learned/inferred.

We hope our work stimulates further investigations along the above avenues.

Acknowledgments

We thank Prof. Shreyas Sundaram (Purdue University), Prof. Philip Paré (Purdue University) and Dr. Bala Kameshwar Poolla (NREL) for helpful discussions.

References

- Manindra Agrawal, Madhuri Kanitkar, and M. Vidyasagar. Modelling the spread of the sars-cov-2 pandemic - Impact of lockdowns & interventions. Technical report, Working paper, 2020.
- Santosh Ansumalia, Shaurya Kaushal, Alope Kumar, Meher K. Prakash, and M. Vidyasagar. Modelling a pandemic with asymptomatic patients, impact of lockdown and herd immunity, with applications to sars-cov-2. Technical report, Working paper, 2020.
- Chris T Bauch and David JD Earn. Vaccination and the theory of games. *Proceedings of the National Academy of Sciences of the United States of America*, 101(36):13391–13394, 2004.
- Sheryl L Chang, Mahendra Piraveenan, Philippa Pattison, and Mikhail Prokopenko. Game theoretic modelling of infectious disease dynamics and intervention methods: A review. *Journal of Biological Dynamics*, 14(1):57–89, 2020.
- Samuel Cho. Mean-field game analysis of SIR model with social distancing. *arXiv preprint arXiv:2005.06758*, 2020.

- Wongyeong Choi and Eunha Shim. Optimal strategies for vaccination and social distancing in a game-theoretic epidemiologic model. *Journal of theoretical biology*, 505:110422, 2020.
- Olivier Coibion, Yuriy Gorodnichenko, and Michael Weber. The cost of the COVID-19 crisis: Lockdowns, macroeconomic expectations, and consumer spending. Technical report, National Bureau of Economic Research, 2020.
- Matz Dahlberg, Per-Anders Edin, Erik Grönqvist, Johan Lyhagen, John Östh, Alexey Siretskiy, and Marina Toger. Effects of the COVID-19 pandemic on population mobility under mild policies: Causal evidence from Sweden. *arXiv preprint arXiv:2004.09087*, 2020.
- Krishna Dasaratha. Virus dynamics with behavioral responses. *arXiv preprint arXiv:2004.14533*, 2020.
- Jessica Enright and Rowland Raymond Kao. Epidemics on dynamic networks. *Epidemics*, 24: 88–97, 2018.
- Eli P Fenichel, Carlos Castillo-Chavez, M Graziano Ceddia, Gerardo Chowell, Paula A Gonzalez Parra, Graham J Hickling, Garth Holloway, Richard Horan, Benjamin Morin, Charles Perrings, et al. Adaptive human behavior in epidemiological models. *Proceedings of the National Academy of Sciences*, 108(15):6306–6311, 2011.
- Jacob K Goeree, Charles A Holt, and Thomas R Palfrey. Quantal response equilibrium and over-bidding in private-value auctions. *Journal of Economic Theory*, 104(1):247–272, 2002.
- Jacob K Goeree, Charles A Holt, and Thomas R Palfrey. Stochastic game theory for social science: A primer on quantal response equilibrium. In *Handbook of Experimental Game Theory*. Edward Elgar Publishing, 2020.
- Google. Covid-19 community mobility reports, 2020. URL <https://www.google.com/covid19/mobility/>. Accessed: 2020-10-26.
- William Greene. Discrete choice modeling. In *Palgrave handbook of econometrics*, pages 473–556. Springer, 2009.
- Philip A Haile, Ali Hortaçsu, and Grigory Kosenok. On the empirical content of quantal response equilibrium. *American Economic Review*, 98(1):180–200, 2008.
- Herbert W Hethcote. The mathematics of infectious diseases. *SIAM Review*, 42(4):599–653, 2000.
- Ashish R Hota and Kavish Gupta. A generalized SIS epidemic model on temporal networks with asymptomatic carriers and comments on decay ratio. *arXiv preprint arXiv:2008.00826*, 2020.
- Ashish R Hota and Shreyas Sundaram. Game-theoretic vaccination against networked SIS epidemics and impacts of human decision-making. *IEEE Transactions on Control of Network Systems*, 6(4):1461–1472, 2019a.
- Ashish R Hota and Shreyas Sundaram. Game-theoretic protection against networked SIS epidemics by human decision-makers. *IFAC-PapersOnLine*, 51(34):145–150, 2019b.
- Ashish R Hota, Jaydeep Godbole, Pradhuman Bhariya, and Philip E Paré. A closed-loop framework for inference, prediction and control of SIR epidemics on networks. *arXiv preprint arXiv:2006.16185*, 2020.

- Yunhan Huang and Quanyan Zhu. A differential game approach to decentralized virus-resistant weight adaptation policy over complex networks. *IEEE Transactions on Control of Network Systems*, 7(2):944–955, 2020.
- A-R Lagos, I Kordonis, and GP Papavassilopoulos. Games of social distancing during an epidemic: Local vs statistical information. *arXiv preprint arXiv:2007.05185*, 2020.
- R Duncan Luce. *Individual choice behavior: A theoretical analysis*. Courier Corporation, 1958.
- Naoki Masuda and Petter Holme. *Temporal network epidemiology*. Springer, 2017.
- Richard D McKelvey and Thomas R Palfrey. Quantal response equilibria for normal form games. *Games and economic behavior*, 10(1):6–38, 1995.
- Wenjun Mei, Shadi Mohagheghi, Sandro Zampieri, and Francesco Bullo. On the dynamics of deterministic epidemic propagation over networks. *Annual Reviews in Control*, 44:116–128, 2017.
- Matthieu Nadini, Alessandro Rizzo, and Maurizio Porfiri. Epidemic spreading in temporal and adaptive networks with static backbone. *IEEE Transactions on Network Science and Engineering*, 7(1):549 – 561, 2020.
- Mark Newman. *Networks: An Introduction*. Oxford University Press, 2010.
- Cameron Nowzari, Victor M Preciado, and George J Pappas. Analysis and control of epidemics: A survey of spreading processes on complex networks. *IEEE Control Systems*, 36(1):26–46, 2016.
- Masaki Ogura, Victor M Preciado, and Naoki Masuda. Optimal containment of epidemics over temporal activity-driven networks. *SIAM Journal on Applied Mathematics*, 79(3):986–1006, 2019.
- Jasmina Omic, Ariel Orda, and Piet Van Mieghem. Protecting against network infections: A game theoretic perspective. In *IEEE INFOCOM 2009*, pages 1485–1493, 2009.
- Maria Pachetti, Bruna Marini, Fabiola Giudici, Francesca Benedetti, Silvia Angeletti, Massimo Ciccozzi, Claudio Masciovecchio, Rudy Ippodrino, and Davide Zella. Impact of lockdown on COVID-19 case fatality rate and viral mutations spread in 7 countries in europe and north america. *Journal of Translational Medicine*, 18(1):1–7, 2020.
- Philip E Paré, Carolyn L Beck, and Angelia Nedić. Epidemic processes over time-varying networks. *IEEE Transactions on Control of Network Systems*, 5(3):1322–1334, 2017.
- Philip E Paré, Carolyn L Beck, and Tamer Başar. Modeling, estimation, and analysis of epidemics over networks: An overview. *Annual Reviews in Control (To appear)*, 2020a.
- Philip E Paré, Ji Liu, Carolyn L Beck, Barrett E Kirwan, and Tamer Başar. Analysis, estimation, and validation of discrete-time epidemic processes. *IEEE Transactions on Control Systems Technology*, 28(1):79–93, 2020b.
- Romualdo Pastor-Satorras, Claudio Castellano, Piet Van Mieghem, and Alessandro Vespignani. Epidemic processes in complex networks. *Reviews of Modern Physics*, 87(3):925, 2015.
- Nicola Perra, Bruno Gonçalves, Romualdo Pastor-Satorras, and Alessandro Vespignani. Activity driven modeling of time varying networks. *Scientific reports*, 2:469, 2012.

- Timothy C Reluga. Game theory of social distancing in response to an epidemic. *PLoS Comput Biol*, 6(5):e1000793, 2010.
- Marguerite Robinson and Nikolaos I Stilianakis. A model for the emergence of drug resistance in the presence of asymptomatic infections. *Mathematical biosciences*, 243(2):163–177, 2013.
- Leonardo Stella, Alejandro Pinel Martínez, Dario Bauso, and Patrizio Colaneri. The role of asymptomatic individuals in the Covid-19 pandemic via complex networks. *arXiv preprint arXiv:2009.03649*, 2020.
- George Theodorakopoulos, Jean-Yves Le Boudec, and John S Baras. Selfish response to epidemic propagation. *IEEE Transactions on Automatic Control*, 58(2):363–376, 2013.
- Stojan Trajanovski, Fernando A Kuipers, Yezekael Hayel, Eitan Altman, and Piet Van Mieghem. Designing virus-resistant, high-performance networks: A game-formation approach. *IEEE Transactions on Control of Network Systems*, 5(4):1682–1692, 2018.
- Piet Van Mieghem. The N-intertwined SIS epidemic network model. *Computing*, 93(2-4):147–169, 2011.
- Lorenzo Zino, Alessandro Rizzo, and Maurizio Porfiri. An analytical framework for the study of epidemic models on activity driven networks. *Journal of Complex Networks*, 5(6):924–952, 2017.
- Lorenzo Zino, Alessandro Rizzo, and Maurizio Porfiri. Analysis and control of epidemics in temporal networks with self-excitement and behavioral changes. *European Journal of Control*, 54:1 – 11, 2020a.
- Lorenzo Zino, Alessandro Rizzo, and Maurizio Porfiri. On assessing control actions for epidemic models on temporal networks. *IEEE Control Systems Letters*, 4(4):797–802, 2020b.